Altered γ-secretase activity in mild cognitive impairment and Alzheimer's disease

軽度認知障害・アルツハイマー病における脳内γ-secretase 活性の変化

角田　伸人

Contents

Abstract

Amyloid β-protein (Aβ) 42 and 43 are converted by stepwise processing by γ-secretase mainly to Aβ38 and 40, respectively. This stepwise processing model was confirmed by LC-MS/MS using the CHAPSO-solubilized γ-secretase assay system I previously established. This assay system showed high specific activity and revealed unusual enzymatic characteristics of γ-secretase. I sought to obtain based on the stepwise processing model a further insight into the mechanism why cerebrospinal fluid (CSF) Aβ42 are lower in Alzheimer's disease (AD) patients and how other Aβ species are. Because Aβ38/42 and Aβ40/43 are distinct product/precursor pairs, these four species in the CSF together should faithfully reflect the status of brain γ-secretase activity and were quantified by specific enzyme-linked immunosorbent assays in the CSF from controls and mild cognitive impairment (MCI)/AD patients. Decreases in the levels of the precursors, Aβ42 and 43, in MCI/AD CSF tended to accompany increases in the levels of the products, Aβ38 and 40, respectively. The ratios Aβ40/43 vs Aβ38/42 in CSF (each representing cleavage efficiency of Aβ43 or Aβ42) were largely proportional to each other but higher in MCI/AD patients compared to control subjects. These data suggest that γ-secretase activity in MCI/AD patients is enhanced at the

conversion of Aβ43 and 42 to Aβ40 and 38, respectively. Consequently, I measured the activity of raft-associated γ-secretase isolated from control as well as MCI/AD brains and found the same, significant alterations (so called modulation) in the γ-secretase activity in MCI/AD brains. Thus I clearly showed that MCI and AD are associated with the changes in γ-secretase activity in the brain.

The thesis consists of two parts: i) establishment of the CHAPSO-solubilized γ-secretase assay system, ii) measurement of human CSF samples and raft-associated γ-secretase activity in human brains.

Introduction

Senile plaques, the neuropathological hallmark of Alzheimer's disease (AD), are composed of amyloid β-protein (Aβ). Aβ is derived from β-amyloid precursor protein (APP) through sequential cleavage by β- and γ-secretases. β-Secretase cleaves at the luminal portion (β-site) of APP to generate β-carboxyl terminal fragment of APP (βCTF), an immediate substrate of γ-secretase, to produce various Aβ species (Fig. 1; Selkoe, 2001). The most abundant secreted species is Aβ40, whereas the species that has two extra residues (Aβ42) is a minor one (< 10%); however, the latter is the species that deposits first and predominates in senile plaques (Iwatsubo et al, 1994).

Presenilin (PS) 1/2 make up the catalytic site of γ-secretase (Fig. 2; Takasugi et al, 2003). The enzymatic properties of γ-secretase that cleave the transmembrane domain of βCTF have been an enigma, although recent studies provided partial elucidation of this mechanism (Qi-Takahara et al, 2005; Takami et al, 2009). To reconstitute γ-secretase activity, membrane was solubilized and membrane lipids were replaced with detergent CHAPSO (Kakuda et al, 2006). This reconstituted γ-secretase activity was similar in many aspects to cell-free γ-secretase activity previously reported by my colleagues (Gu et al, 2001; Sato et al, 2003). Recently, Takami et al proposed

'stepwise processing model' using the reconstituted γ-secretase assay system (Takami et al, 2009). γ-Secretase has two Aβ product lines, which successively convert Aβ49 and Aβ48 that are generated by ε-cleavage, to shorter Aβs by releasing tri- or tetrapeptides in a stepwise fashion. Aβ49 is successively cleaved mostly into Aβ40 via Aβ46 and Aβ43, while Aβ48 is similarly cleaved into Aβ38 via Aβ45 and Aβ42 (see Fig. 11). Importantly, the differences between the amounts of released tri- and tetrapeptides at each step determine the levels of various Aβ species produced (Takami et al, 2009). Thus, the true activity of γ-secretase is defined by the amounts of tri- and tetrapeptides released, but not by the amounts of Aβ species produced. Of note, the most abundant species Aβ40 is derived not from Aβ42, but from Aβ43. Also Aβ38 is derived mainly from Aβ42 (Fig. 11). The longer Aβs in CSF including Aβ49 and 46 as well as Aβ48 and 45 must be generated at negligible levels, but may neither be secreted to the interstitial fluid (ISF) nor recruited to CSF. This suggests that the status of brain, and possibly neuronal, γ-secretase could be accurately assessed by measuring all four Aβ species generated by the two product lines of γ-secretase.

To measure each Aβ in CSF, I established new enzyme-linked immunosorbent assays (ELISAs). Using these ELISAs, I quantified Aβ40 and 43 and Aβ38 and 42 in

CSF samples from control subjects and MCI/AD patients. The CSF concentrations of Aβ43 and Aβ42 were found to be significantly lower in MCI/AD compared with control. The ratio of Aβ38/42, which represents the ratio of product/precursor and thus the cleavage efficiency of Aβ42, was plotted against the ratio of Aβ40/43, which represents the ratio of product/precursor in the other product line and thus the cleavage efficiency of Aβ43. The ratio of Aβ38/42 was largely proportional to that of Aβ40/43, indicating that the two cleavage processes are tightly coupled, but both were generally higher in MCI/AD patients compared to control subjects These results suggest that the activity of brain γ-secretase in MCI/AD is enhanced at the conversion of Aβ43 to Aβ40 and Aβ42 to Aβ38, which would result in significantly lower CSF concentrations of Aβ42 and 43. In support of this hypothesis, the activities of raft-associated γ-secretase from control and MCI/AD brains were found to significantly differ from each other: although the total Aβ production was similar, the γ-secretase in MCI/AD brains produced significantly larger ratios of Aβ40/43 and Aβ38/42 than the enzyme in control brains. This raises the possibility that lower CSF levels of Aβ42 and 43 simply reflect the altered γ-secretase activity in the MCI/AD-affected brains.

Materials and methods

Cell culture

Chinese hamster ovary (CHO) cells were cultured in Dulbecco-modified Eagle's medium (Sigma, St. Louis, MO) containing 10% fetal bovine serum (Invitrogen, Carlsbad, CA) and penicillin/streptomycin (Invitrogen). CHO cells expressing human wild type (wt) or mutant (mt) PS1/2 were generated as described by Yagishita et al (2006). Displacement of endogenous (hamster) PS by exogenous (human) PS was confirmed in each cell line (Yagishita et al, 2006).

Preparation of C99-FLAG substrate

A carboxyl terminal fragment of APP (C99) was C-terminally fused with FLAG tag (C99-FLAG) and N-terminally with signal peptide (MQLRNPELHLGCALALRFLALVSWDIPGARA) of human α-galactosidase A. Resultant fragment was inserted into pFASTBAC™ 1 (Invitrogen). Sf9 cells were infected with recombinant baculovirus according to the manufacturer's instructions. Infected cells (60 ml culture) were harvested after 36 h and resuspended in 0.3 - 0.5 ml of Tris-buffered saline (50 mM Tris HCl, pH 7.6, 150 mM NaCl). The suspension was

mixed with equal amount of lysis buffer [50 mM Tris HCl, pH 7.6, 150 mM NaCl, 2% NP-40 and 2 x protease inhibitor cocktail (Roche Diagnostics, Indianapolis, IN)] and incubated on ice for 1 h. After ultracentrifugation at 245,000 x g for 20 min, the supernatant was agitated with 0.2 ml of ANTI-FLAG® M2 agarose beads (Sigma) overnight. C99-FLAG was eluted from the beads by incubation with 0.2 ml of 100 mM Glycine HCl (pH 2.7) for 10 min at room temperature, and the eluate was immediately neutralized by addition of 1/25 volume of 1 M Tris HCl (pH 8.0). Concentrations of residual NP-40 in purified C99-FLAG were estimated to be 0.3 – 0.4% from elution volume. The eluted C99-FLAG was confirmed for its purity and quantified by CBB staining after gel electrophoresis.

γ-Secretase assay and detection of Aβ and AICD

Microsomal fractions of CHO cells were obtained as previously described (Funamoto et al, 2004). Briefly, the harvested cells were homogenized in buffer A (20 mM PIPES, pH 7.0, 140 mM KCl, 0.25 M sucrose, 5 mM EGTA) using a glass/Teflon homogenizer. The homogenates were centrifuged at 800 x g for 10 min to remove nuclei and cell debris. The postnuclear supernatants were recentrifuged at 100,000 x g

for 1 h. The resulting pellets representing the microsomal fractions were suspended in a buffer (50 mM PIPES, pH 7.0, 0.25 M sucrose, 1 mM EGTA). Their protein concentrations were adjusted at 10 mg/ml. The membranes were solubilized by the addition of equal volume of 2 x NK buffer [50 mM PIPES, pH 7.0, 0.25 M sucrose, 1 mM EGTA, 2% CHAPSO (Sigma; Cat NO. C3649; lot #, 013K5314 and 015K5313), 2 mM DIFP, 20 μg/ml antipain, 20 μg/ml leupeptin, 20 μg/ml TLCK, 10 mM phenanthroline and 2 mM thiorphan] and incubated on ice for 1 h (Li et al, 2000; Fraering et al, 2004). After centrifugation at 100,000 x g for 1 h, the supernatants were saved (1% CHAPSO lysate). 1% CHAPSO lysate was diluted with three volumes of CHAPSO-free buffer (50 mM PIPES, pH 7.0, 0.25 M sucrose, 1 mM EGTA, 1 mM DIFP, 10 μg/ml antipain, 10 μg/ml leupeptin, 10 μg/ml TLCK, 5 mM phenanthroline and 1 mM thiorphan) containing defined amounts of C99-FLAG. Furthermore, 0.1% phosphatidylcholine (Sigma; Cat NO. P3556; lot #, 034K5218) was added into the diluted lysate, which significantly enhanced the activity of γ-secretase but did not alter the proportion of Aβ40/42 produced. Residual NP-40 in the substrate should be estimated carefully before starting reaction. The NP-40 concentrations at 0.2% and above in the reaction mixture abolished γ-secretase activity. Its final concentrations in

all reactions in this study were kept less than 0.06%, which exhibited no noticeable suppression in Aβ and AICD productions. After incubation at 37ºC for 3 h, lipids were extracted with chloroform/methanol (2:1), and protein residues were subjected to quantitative western blotting with defined amounts of synthetic Aβ as a control. For AICD standard, I used CTF50 synthetic peptide (AICD50-99; Calbiochem, San Diego, CA) or AICD50-99-FLAG expressed in *E. coli* as described below. For detection of Aβ, 82E1, a monoclonal antibody end-specific for N-terminus of human Aβ (IBL, Gunma, Japan) was used (Horikoshi et al, 2004). To visualize APP intracellular domain (AICD), UT-421 (gift of Dr. T. Suzuki, Hokkaido University) raised against C-terminal sequence of APP was used (Tomita et al, 1998). All blots in this study were immersed in boiled PBS for 5 min before blocking in 5% skim milk, which profoundly enhanced detectability of the antigens.

Quantification of authentic AICD50-99-FLAG

AICD50-99-FLAG was expressed in *E. coli* and affinity-purified with ANTI-FLAG M2 beads®. The protein concentrations of authentic AICD50-99-FLAG were determined using both amino acid compositional analysis that determines the total

protein amount, and sequence analysis that assesses the amount of AICD50-99-FLAG. The appropriate amounts of AICD50-99-FLAG were purified by reverse-phase liquid chromatography on super-phenyl column (Tosoh, Tokyo, Japan) with 0-48% gradient of acetonitrile in 0.1% trifluoroacetic acid. Peak fractions were collected and rechromatographed under the same condition. Compared between the peak areas of first and second chromatogram, the recovery from chromatography was estimated about 58%. Pooled fractions from the second chromatography were dried and hydrolyzed in 6 N HCl vapor at 110˚C for 20 h. The acid hydrolyzate was derivatized with 6-aminoquinolyl-N-hydroxysuccinimidyl carbamate and quantified as described by Shindo et al (1997). For amino acid sequence analysis, an appropriate amount of AICD-FLAG was subjected to Edman degradation using a Procise cLC protein sequencing system (Applied Biosystems, Foster City, CA) to obtain N-terminal 10-residue sequence. Repetitive yield and initial yield were calculated from the sequence.

Detection of longer Aβs produced by γ-secretase

Various longer Aβ species were separated on a Tris/Tricine/8 M urea gel with minor

modifications (Yagishita et al, 2004; Qi-Takahara et al, 2005). A 10% T/3% C separation gel, pH 8.45, containing 8 M urea (gel system I) was used to separate Aβ37 through Aβ45. A 12% T/3% C separation gel, pH 8.90, containing 8M urea (gel system II) was used to separate Aβ46 through Aβ49. The spacer and stacking gels did not contain urea. Following transfer, the blots were probed with 82E1 to detect only Aβs that begin at Asp-1 and developed using an ECL system. Intensities of the bands were quantified using a LAS-1000plus luminescent image analyzer (Fuji Film, Tokyo, Japan).

Immunoprecipitation of γ-secretase

1% CHAPSO lysate of mouse embryonic fibroblasts (MEF) or wt or mtPS1-transfected CHO cells was diluted in three volumes of CHAPSO-free buffer (Nyabi et al, 2002). γ-Secretase complex was immunoprecipitated with anti-nicastrin antibody (Sigma) and Protein G-Sepharose (Amersham biotech, Uppsla, Sweden). After sufficient washing with 0.25% CHAPSO buffer (50 mM PIPES, pH 7.0, 250 mM sucrose, 1 mM EGTA, 0.25% CHAPSO, 1 mM DIFP, 10 μg/ml antipain, 10 μg/ml leupeptin, 10 μg/ml TLCK, 5 mM phenanthroline and 1 mM thiorphan), γ-secretase

complex bound to protein G-Sepharose was allowed to react with 500 nM C99-FLAG in 0.25% CHAPSO buffer containing 0.1% phosphatidylcholine at 37 ºC for 4 h with gentle agitation. The reaction mixtures were subjected to quantitative western blotting for Aβ and AICD (Yagishita et al, 2006; Qi-Takahara et al, 2005).

Mass spectrometric analysis of AICDs

After incubating 0.25% CHAPSO lysate of CHO cells with C99-FLAG in the presence of 0.1 mM bestatin, 10 μM amastatin, 0.1 μM arphamenine A, the uncleaved excess C99-FLAG was largely removed by immunoprecipitation with 4G8, a monoclonal antibody raised against 17-28 residues of Aβ (epitope:17-24 residues) (Signet Laboratories, Dedham, MA). Produced AICD was immunoprecipitated with ANTI-FLAG® M2 agarose beads, and extracted with 30% acetonitrile in 1% trifluoroacetate. Masses of the peptides were determined with a MALDI-TOF mass spectrometer, autoflex® (Bruker Daltonics, Ibaraki, Japan). Samples were prepared by the thin-layer method using sinapinic acid as a matrix (Sato et al, 2003).

Subjects.

CSF samples from 24 AD patients (mild to moderate AD; 50-86 years old), 19 MCI patients (amnestic MCI; 57-82 years old), and 21 control subjects (61-89 years old) were collected (see Table 3) at Department of Neurology, Hirosaki University School of Medicine and Hospital and at Department of Geriatrics and Gerontology, Tohoku University Hospital, and at Department of Neurology, Niigata University Medical and Dental Hospital. The CSF samples from (symptomatic) 5 FAD (mPS1) patients (T116N, L173F, G209R, L286V and L381V) were from Niigata University Medical and Dental Hospital. Probable AD cases met the criteria of the National Institute of Neurological and Communicative Disorders and Stroke-Alzheimer's Disease and Related Disorders (NINCDS-ADRDA) (McKhann et al, 1984; Kuwano et al, 2006); this criteria consist of i) Dementia established by examination and objective testing, ii) Deficits in two or more cognitive areas, iii) Progressive worsening of memory and other cognitive functions, iv) No disturbance in consciousness, v) Onset between ages 40 and 90. Diagnosis of amnestic MCI criteria consist of i) Memory complaint preferably corroborated by an informant ii) Objective memory impairment for age iii) Largely preserved general cognition iv) Essentially normal activities of daily living v)

Not demented (Petersen et al, 2001; Winblad et al, 2004). Additional diagnostic procedures included magnetic resonance imaging. Dementia severity was evaluated by the Mini-Mental State Examination (MMSE). MMSE score is 24 to 30 for amnestic MCI and control, 21 to 26 for mild AD, and 10 to 20 for moderate AD (tentatively defined). Diagnosis of idiopathic normal pressure hydrocephalus (iNPH) was made according to the guideline issued by the Japanese Society of NPH (Ishikawa et al, 2008). Controls who had no sign of dementia and lived in an unassisted manner in the local community were recruited. All individuals included in this study were Japanese and 24 AD patients examined here were judged to have sporadic AD because of negative family history. This study was approved by the ethics committee at each hospital or institute.

Human cortical specimens for quantification of raft-associated γ-secretase activity were obtained from those brains that were removed, processed and placed in -80˚C within twelve hours postmortem [Patients were placed in a cold (4˚C) room within 2h after death] at the Brain Bank at Tokyo Metropolitan Institute of Gerontology. For all the brains registered at the bank my corroborators obtained written informed consents for their use for medical research from patient or patient's family. Each brain specimen

(~0.5g) were taken from Brodmann areas 9-11 of 13 AD patients [80+/-5.0 years of age, Braak NFT stage>IV, SP stage=C, (retrospective) CDR >1], 10 MCI patients (91+/-4.9 years of age, Braak NFT stage <IV, SP stage<C, CDR=0.5) and 16 controls (77+/-6.5 years of age, Braak NFT stage<I, SP stage=0/A, CDR=0). The diagnoses of AD, MCI and control were made according to the published criteria (Li et al, 1997; Adachi et al, 2010).

Cerebrospinal fluid analysis.

CSF (10-15 ml) was collected in a polypropylene or polystyrene tube and gently inverted. After brief centrifugation CSF was aliquoted to polypropylene tubes (0.25-0.5 ml), which were kept at -80 ˚C until use. In my experience, Aβ42 (possibly, other Aβ species too) are readily absorbed even to polypropylene tubes (~20% per new exposure, as shown by Luminex xMAP quantification), and repeated aliquot to new tubes may cause profoundly lower measures of Aβs (T Tsukie and R Kuwano, unpublished data, 2010). This may partly explain why absolute levels of Aβs in CSF greatly vary across laboratories, whereas their relative ratios (for example, Aβ42/40) seem to be roughly consistent. The CSF concentrations of Aβ38, 40, 42 and 43 were

quantified using commercially available ELISA kits (Cat NO. 27717, 27718, 27712, 27710, respectively, IBL, Gunma, Japan).

CSF immunoprecipitation and Western blotting.

When required, CSF Aβs were immunoprecipitated with protein G-Sepharose conjugated with 82E1 at 4˚C by keeping a container in gentle rotation overnight. The mixture was centrifuged at 10,000 x g for 5 minutes, and resultant pellets were then washed twice with phosphate-buffered saline. The washed beads were suspended with the Laemmli sample buffer for SDS-PAGE. The immunoprecipitated Aβs were separated on Tris/Tricine/8 M urea gels (Kakuda et al, 2006), followed by Western blotting using 82E1. To immunodetect Aβ42 and Aβ43, Aβ42 monoclonal antibody (44A3, IBL) and Aβ43 polyclonal antibody (IBL) were used (Fig. 10).

Quantification of human brain raft-associated γ-secretase activity.

Since γ-secretase is thought to be concentrated in rafts (Wada et al, 2003; Hur et al, 2008), I measured raft-associated γ-secretase activity rather than CHAPSO-solubilized activity. Rafts were prepared from human brains, which were frozen within 12h postmortem, as previously described (Oshima et al, 2001; Wada et al, 2003) with some

modifications. I do not know exactly whether the γ-secretase activity depends upon the sampling site. In my hand, there appear no large differences in the activity among the sampled sites in a given prefrontal slice. No significant differences in the activity were noted between outer and inner layer of the cortex. After carefully removing leptomeninges and blood vessels, small (<0.5 g) cortical blocks from prefrontal cortices (Brodmann areas 9 to 11) were homogenized in ~10 volumes of 10% sucrose in MES-buffered saline (25 mM MES, pH 6.5, and 150 mM NaCl) containing 1% CHAPSO and various protease inhibitors. The homogenate was adjusted to 40% sucrose by the addition of an equal volume of 70% sucrose in MES-buffered saline, placed at the bottom of an ultracentrifuge tube, and overlaid with 4 ml of 35% sucrose and finally with 4 ml of 5% sucrose in MES-buffered saline. The discontinuous gradient was centrifuged at 39,000 rpm for 20h at 4˚C on a SW 41 Ti rotor (Beckman, Palo Alto, CA). An interface of 5%/35% sucrose (fraction 2) was carefully collected (referred to as raft fraction). Raft fractions were recentrifuged after dilution with buffer C (20 mM PIPES, pH 7.0, 250 mM sucrose and 1 mM EGTA). The resultant pellet was washed twice and resuspended with buffer C, which was kept at -80˚C until use.

As the method of quantifying the raft γ-secretase activity was not yet established,

I first determined the assay conditions. The incubation of raft fraction with βCTF generated exactly the same tri- and tetrapeptides my colleagues previously observed in the detergent-soluble γ-secretase assay system (Takami et al, unpublished observation). This suggests that the cleavage by raft-associated γ-secretase proceeds in the identical manner as by CHAPSO-reconstituted γ-secretase (Takami et al, 2009). In my hand, preexisting βCTF bound in rafts generated only negligible amounts of Aβs, and their generation was dependent exclusively on exogenously added βCTF. Thus, I concluded that the addition of βCTF to raft fraction make possible to measure the raft-associated γ-secretase activity, although I do not know how the exogenously added βCTF is integrated into raft, gets access to and is degraded by raft-embedded γ-secretase. Using this assay method, the activities of raft-associated γ-secretase in human brains were found to be only a little affected postmortem, when compared with that prepared from fresh rat brains. A progressive decline in the activity was barely detectable from 4 to 17h postmortem. The discrepancy in the postmortem decay between my and the previous data (Hur et al, 2008) would be ascribed to the assay method: The latter are based on the activity measured by using endogenous (raft-bound) substrate that is also susceptible to proteolytic degradation (Hur et al, 2008).

Each raft fraction, adjusted to 100 μg/ml in protein concentration, was incubated with 200 nM C99FLAG for 2h at 37˚C (Kakuda et al, 2006). The produced Aβs were separated on SDS-PAGE, and subjected to quantitative Western blotting, using specific antibodies, 3B1 for Aβ38, BA27 for Aβ40, 44A3 for Aβ42 and anti- Aβ43 polyclonal for Aβ43.

Statistical analysis.

All statistical analyses were performed using SPSS version 14.0. The results were expressed as means ± standard deviations. Because data transformations were required to achieve normal distribution, all analyses including Aβ38, Aβ40, Aβ42 and Aβ43 were performed after a logarithmic transformation. Pearson's correlation coefficients were calculated to indicate the strength of the linear relationship between two variables. An analysis of variance (ANOVA) was used to test the equality of means of continuous variables among three groups, that is, control, MCI and AD. Multiple comparisons were done by Dunnett's t-test, Bonferroni's t-test and Welch's t-test between control and MCI/AD, and among three groups, respectively. A three-tailed P of <0.05 was considered to be statistically significant.

Results

I. Establishment of CHAPSO-solubilized γ-secretase assay system.

CHAPSO-solubilized γ-secretase assay system—Relationship between γ-cleavage and APP intracelluar domain (AICD) production had been a matter of debate. Studies by a number of research groups implied that γ-cleavage was largely independent of ε-cleavage (Chen et al, 2002; Moehlmann et al, 2002; Hecimovic et al, 2004; Jankowsky et al, 2004). On the other hand, Pinnix et al noted a potential link between Aβ and AICD productions (Pinnix et al, 2001). Recently, my colleagues and others (Sato et al, 2003; Funamoto et al, 2004; Zhao et al, 2005) identified novel ε-cleavage that liberates AICD and assumed that ε-cleavage was the primary event for Aβ production. They also assumed that equal amount of total Aβ and AICD are produced by γ-secretase. Most of quantitative studies on Aβ and AICD productions were performed in the presence of large amounts of αCTF, which is processed to p3 and AICD, but not to Aβ. In addition, levels of Aβ and AICD were assessed by methods based on different principles, such as ELISA for Aβ released into media and indirect luciferase transactivation assay for AICD. To my knowledge, rigorous quantitative determination by conventional western blotting of the produced Aβ and

AICD had never been performed.

To examine the stoichiometry of Aβ relative to AICD, I took the advantage of the CHAPSO-solubilized γ-secretase assay system (Li et al, 2000; Fraering et al, 2004). C99 was fused at the C-terminus with FLAG tag (C99-FLAG), which was expressed in Sf9 cells. After C99-FLAG was purified by ANTI-FLAG M2 (see Materials and Methods), its purity was confirmed and its amounts were quantified by CBB staining (see Fig. 4B). Purified 0.5 μM C99-FLAG was incubated in 0.25% CHAPSO-lysate of CHO cells. Produced Aβs were separated on gel system I (Yagishita et al, 2006; Qi-Takahara et al, 2005) (Fig. 3A). The amount of each Aβ species increased in a time-dependent linear fashion and was assesed by densitometric scanning of the western blot. Robust signals for Aβ42 and Aβ43 were detected as well as for Aβ40, which contrasts with the major Aβ species in cell-based and cell-free assays (Selkoe, 2001; Sato et al, 2003; Qi et al, 2003; Hayashi et al, 2004) (Fig. 3A). Aβ45, and Aβ species longer than Aβ45 were also detected and stuck at the bottom of gel (Fig. 3A, upper panel). Gel system II (Yagishita et al, 2006; Qi-Takahara et ak, 2005) revealed that these longer species were Aβ48 and Aβ49 (Fig. 3A). Against increasing concentrations of C99-FLAG, band intensities of all Aβ species were plotted as

percentage of intensity of synthetic Aβ45 (50 pg) on each blot (Fig. 3B and C). The production rates of all Aβ species followed Michaelis-Menten type curve (Fig. 3C). The apparent *K*m (*K*app) and *V*max values for various Aβ species were summarized in Table 1. As can be seen in Figure 3A and 3B, this solubilized γ-secretase assay system was characterized by production of abundant Aβ40, Aβ42 and Aβ43, and small or trace amounts of Aβ45, Aβ48, and Aβ49. The majority of Aβ species produced by the assay system consisted of Aβ40, Aβ42 and Aβ43 (see below).

In this assay system L-685,485 and DAPT suppressed Aβ production in a dose-dependent manner (Fig. 3D and E). As expected, L-685,485, a transition-state analogue inhibitor, uniformly suppressed production of all Aβ species (Fig. 3D). Most unexpectedly, DAPT, a nontransition-state analogue inhibitor, did not cause a build-up of Aβ43 and Aβ46 (Yagishita et al, 2006; Qi-Takahara et al, 2005; Zhao et al, 2004; Zhao et al, 2005), but uniformly suppressed the production of all Aβ species (Fig. 3E). This may indicate that membrane integrity is a prerequisite for DAPT-induced accumulation of Aβ43 and Aβ46, as this phenomenon was observed in cell-based assay (Qi-Takahara et al, 2005) and cell-free assay using microsomal fraction.

Stoichiometric relationship between Aβ and AICD—Purified C99-FLAG was

incubated with CHAPSO-solubilized microsomal fraction from CHO cells. The Aβ at about 4 kDa on the SDS gel was quantified by western blotting as previously reported (Funamoto et al, 2004). Total AICD was quantified using synthetic CTF50 (AICD50-99, eight residues smaller than the substrate, AICD-FLAG) as an authentic sample. The highest molecular mass band at about 15 kDa and lowest-molecular-mass band at about 9 kDa, before incubation represent presumably N-terminally extended C99-FLAG with residual signal peptide and truncated C99-FLAG, respectively (Fig. 4A, lower panel). CBB staining cannot detect those fragments and thus only trace amounts of the fragments contaminate the substrate (Fig. 4B). The Aβ band at about 4 kDa on the SDS gel most likely represents Aβ40, Aβ42 and Aβ43. Aβs longer than Aβ43 have slower mobilities (data not shown and see ref. Yagishita et al, 2006), and can be separated from the major Aβ band at about 4 kDa. The longer Aβs appear to be present in very small amounts, as they constituted around 10% of the total amount estimated from densitometric scanning of the western blot (gel I; Fig. 3A and Table 1), assuming that the retention efficiency for each Aβ species is equal. Thus, Aβ here indicates virtually the sum of Aβ40, Aβ42, and Aβ43. Time course analysis showed that equal amounts of Aβ and AICD increased similarly in a time-dependent manner

(Fig. 4A and C); the kinetics of Aβ and AICD production was statistically indistinguishable (Fig. 4D). These observations indicate that cleavage of C99 provides equal amounts of Aβ (mostly Aβ40, 42 and 43) and AICD. The rates of Aβ and AICD production apparently followed Michaelis-Menten type curve (Fig. 4D). The apparent *K*m (*K*app) values of C99 for Aβ and AICD production were 507.93 ± 26.45 nM and 468.72 ± 129.26 nM, respectively (Table 2). Those values are roughly consistent with *K*m values reported previously for crude and purified γ-secretase (Li et al, 2000; Fraering et al, 2004; Tian et al, 2002). The apparent *V*max values for Aβ and AICD were 433.53 ± 51.94 pM/min and 419.62 ± 19.39 pM/min, respectively (Fig. 4D and Table 2). Those values were more than 30-fold higher than reported previously (Fraering et al, 2004; Hayashi et al, 2004). Such high activity of γ-secretase in my system made it possible to use conventional western blotting to accurately quantify the amounts of Aβ and AICD produced.

I then examined the stoichiometry between Aβ and AICD in reaction mixtures containing mtAPP and mtPS1/2. The CHAPSO lysates were reacted with C99-FLAG containing FAD mutations T714I, V717F and L723P, and an artificial mutation I716F (I45F, according to Aβ numbering) (Lichtenthaler et al, 1999). As shown in Figure 5A,

the mtAPPs tested in this study caused substantial to profound reductions in Aβ and AICD productions (Fig. 5A). Nevertheless, these mtAPPs did not alter the stoichiometry between Aβ and AICD (Fig. 5B). Similarly, mtPSs led to significantly reduced production of Aβ and AICD, but maintained the one-to-one stoichiometry indicated for wtPS1/2 (Fig. 5C and D). In G384A mtPS1, an additional signal was detected above the Aβ band (Fig. 5C) and identified as a mixture of Aβ48 and Aβ49 on gel II (data not shown). Densitometric analysis showed that the longer Aβs produced by G384A mtPS1 amount to more than 40% of total Aβs, as compared to less than 10% in wtPS1. Signals from longer Aβs were included for the quantification of Aβ in G384A mtPS1. Weak additional signals for longer Aβs were also observed in wtPS2 and N141I mtPS2, and similarly included for the quantification of Aβ (Fig. 5C and D).

Identification of longer Aβs, Aβ48 and Aβ49, produced by γ-secretase—Previous observations by my colleagues on ε-cleavage itself led to predict the two counterparts of AICDs, namely Aβ48 and Aβ49 (Sato et al, 2003). Consistent with this assumption, the cells expressing Aβ48 or Aβ49 secreted Aβ40 and Aβ42 into media in a PS-dependent manner (Funamoto et al, 2004).

By using this solubilized system, I sought to confirm γ-secretase-dependent production of Aβ48 and Aβ49. γ-Secretase complex that has been known to contain mature (highly glycosylated) nicastrin (Kimberly et al, 2002), was immunoprecipitated with anti-nicastrin antibody from 0.25% CHAPSO-solubilized MEF lysate. This partially purified γ-secretase complex was incubated with C99-FLAG, and the reaction mixtures were subjected to gel system II to detect Aβ48 and Aβ49. The immunoprecipitate from wtMEF by anti-nicastrin antibody produced Aβ and AICD from C99-FLAG, whereas that by preimmune serum generated negligible levels of Aβ and AICD (Fig. 6A). Precipitate from PS1/2-deficient MEF contained only an immature form of nicastrin and generated no products (Fig. 6A). Gel II clearly shows the two distinct bands for Aβ48 and Aβ49 in the immunoprecipitate from wtMEF but none in that from PS1/2-deficient MEF (Fig. 6B). Furthermore, Aβ48 and Aβ49 were profoundly reduced by the addition of L-685,458, in a dose-dependent manner (data not shown). These data indicate that γ-secretase does produce Aβ48 and Aβ49 as well as other Aβs. Aβ46 was undetectable in this CHAPSO-solubilized system, for which currently I cannot offer an appropriate explanation (Yagishita et al, 2006; Qi-Takahara et al, 2005; Zhao et al, 2004; Zhao et al, 2005).

Only two AICDs, AICD49-99 and AICD50-99, are produced by γ-secretase—In the cell-free system, two ε-cleavage sites along C99, which released AICD49-99 and AICD50–99, were detected. Despite intensive efforts, I failed to identify any longer AICDs, for example, AICD41-99 and AICD43-99 as potential counterparts of Aβ40 and Aβ42, respectively (Gu et al, 2001; Sato et al, 2003). Because this solubilized system allows free collision of enzyme and substrate in the solution, it is quite possible that various ε-cleavage sites could emerge, generating various lengths of AICDs. If C99-FLAG is cleaved once along its transmembrane domain, various AICDs can be expected as counterparts of various Aβ species. Because Aβ40, Aβ42, and Aβ43 are abundant in the assay system, their counterparts, AICD41-99, AICD43-99, and AICD44-99, should have been abundant.

The CHAPSO lysate of CHO cells was incubated with C99-FLAG at 37˚C. Uncleaved C99-FLAG was removed by the pretreatment with 4G8, and AICD-FLAG was subsequently precipitated with ANTI-FLAG® M2 agarose. The immunoprecipitate was subjected to time-of-flight (TOF) mass spectrometry. Most surprisingly, even under this solubilized condition, only two species of AICD, AICD49-99-FLAG and AICD50-99-FLAG, were detected (Gu et al, 2001; Sato et al, 2003) (Fig. 6C), which

contrasts with the presence of various Aβ species generated, as shown by the gel system I (Fig. 3A).

To confirm further the stoichiometry between Aβ and AICD produced by γ-secretase, immunoprecipitated γ-secretase was used to avoid possible contamination with proteases. In addition, instead of AICD50-99, AICD50-99-FLAG expressed in *E. coli* was used as strict control. AICD50-99-FLAG purified from *E. coli* was quantified by amino acid compositional analysis and sequence analysis (see materials and methods). Compared with that purified from wt and M146L mtPS1 cell lysates, the purified γ-secretrase from G384A mtPS1 lysate exhibited profoundly reduced enzymatic activity, as observed in the CHAPSO solubilized membrane (Fig. 6D, left panel). More importantly, purified γ-secretases from three cell lines similarly exhibited one-to-one stoichiometry between Aβ and AICD (Fig. 4D, right panel). Again only two AICD species were detectable (Gu et al, 2001; Sato et al, 2003) (Fig. 6C).

MtPS1/2 and mtAPP are associated with increased proportions of AICD49-99—By using the cell-free assay, Sato et al previously showed increased proportions of AICD49-99 relative to total AICDs in those cells expressing mtAPP or mtPS1/2 (Sato et al, 2003). Here, I reexamined the effect of those mutations on ε-cleavage sites using

the CHAPSO-solubilized assay system. The CHAPSO lysate was incubated with wt or mtC99-FLAG, and subjected to the gel system I (Fig. 7A). T714I mtC99-FLAG remarkably increased the proportion of Aβ42, decreased the proportions of Aβ40 and Aβ43 (Fig. 7A), and released only AICD49-99-FLAG (Fig. 7B). This contrasts with wtC99-FLAG, which produced both AICD49-99-FLAG and AICD50-99-FLAG. With V717F mtC99-FLAG, the abundance of individual Aβ species on gel I was similar to that with wtC99-FLAG, but only AICD49-99FLAG was detected. An artificial mutant, I716F mtC99-FLAG (I45F, according to Aβ numbering), predominantly produced Aβ42, but both AICD49-99-FLAG and AICD50-99-FLAG were detected. No detectable amounts of Aβ and AICD were produced from L723P mtC99-FLAG.

Similarly, the effects of mtPS1/2 on the Aβ and AICD species generated were investigated. As was the case with wtC99-FLAG, wtPS1/2 showed robust production of Aβ42 and Aβ43 (Fig. 8A) and generated AICD49–99-FLAG and AICD50–99-FLAG, with the latter giving a stronger signal (Fig. 8B). Although M146L mtPS1 produced Aβ40 as did wtPS1, M233T and G384A mtPS1 and N141I mtPS2 similarly exhibited an increase in the Aβ42/Aβ40 ratio (Fig. 8A). In addition, it is of note that each mtPS1/2 invariably provides higher signal intensity for

AICD49-99FLAG relative to that for AICD50-99FLAG (Fig. 8B). Most interestingly, M233T mtPS1 produced only AICD49-99-FLAG, as did T714I and V717F mtC99-FLAG (see Fig. 7B). After incubation, the reaction mixture was subjected to the gel system II. Whereas both Aβ48 and Aβ49 were detectable in the wtPS1-containing reaction mixture, only Aβ48 was identified in the M233T mtPS1-containing reaction mixture (Fig. 8C). These observations strongly suggest that Aβ48 is a counterpart of AICD49-99-FLAG that is generated exclusively by M233T mtPS1. These also warrant the accuracy of identification of longer Aβ by the present gel systems.

Recently, Takami et al proposed 'stepwise processing model' using this established CHAPSO-reconstituted assay (Takami et al, 2009). γ-Secretase is assumed to have two product lines, which successively convert the Aβ49 and Aβ48 that are generated by ε-cleavage, to conventional Aβs by releasing tri- or tetrapeptides in a stepwise fashion. Aβ49 is successively cleaved mostly into Aβ40 via Aβ46 and Aβ43, while Aβ48 is similarly cleaved into Aβ38 via Aβ45 and Aβ42. Thus I measured human CSF Aβs using newly established ELISAs on the based the 'stepwise processing model'.

II. Measurement of human CSF samples and raft-associated γ-secretase activity.

ELISA constructions—The plates were coated with each carboxyl terminus–specific antibody. HRP-labeled 82E1 (specific for the amino terminus of human Aβ) was used to detect bound Aβ1-x, except Aβ38 ELISA in which 82E1 is used as the capture with Aβ38 carboxyl terminus–specific HRP-labeled antibody as the detector. ELISAs used here detect Aβ1-x, but not amino-terminally truncated Aβs and now commercially available from IBL as Cat NO. 27717 and 27710. The specificities of ELISAs are provided in Fig. 9.

Measurement of human CSF samples—The CSF samples, from mild to moderate AD and amnestic MCI patients were collected at Department of Neurology, Hirosaki University School of Medicine and Hospital, Department of Geriatrics and Gerontology, Tohoku University Hospital and Department of Neurology, Niigata University Medical and Dental Hospital. The CSF from control, who had no sign of dementia and lived in an unassisted manner in the local community,were collected at above hospitals (see Materials and Methods). The all CSFs were appropriately diluted and quantified with newly established ELISA kits, and the immunoprecipitated Aβs were detected with Western blotting (see materials and methods). All concentrations of

Aβs were in the following order: Aβ40 > Aβ38 > Aβ42 >> Aβ43 in all CSF samples examined (Table 3; see Fig. 10A). This Western blotting pattern appeared not to differ significantly among control, MCI and AD subjects (data not shown). The relative amounts of Aβs were constant across the samples: Aβ38:40 ratio in CSF was ~1:3, and Aβ42:43 ratio was ~10:1. The CSF concentrations of Aβ40 were significantly increased in AD compared to control (Table 3; $P<0.05$, Dunnett's *t*-test). Additionally, the CSF concentrations of Aβ38 tended to be increased in AD patients compared to controls. In contrast, those of Aβ42 and 43 were significantly decreased in MCI/AD compared to controls ($P<0.05$, Dunnett's *t*-test). Although the apolipoprotein ε4 allele is known as the strong risk factor for AD, the CSF concentrations of Aβ species of interest were not influenced by the alleles (data not shown). Interestingly, as reported previously (Schoonenboom et al, 2005), the CSF concentrations of Aβ40 and Aβ38 were proportional to each other in all subjects [Fig. 12A; ln(Aβ40)=0.910 x ln(Aβ38)+1.642, R=0.913, where ln(Aβ40) is the logarithm of Aβ40], even in MCI/AD cases. This was so despite the fact that these species are derived from the two different product lines of γ-secretase (Fig. 11; Takami et al, 2009). In other words, the amounts of products in the third step of cleavage were strictly proportional to each

other across the product lines. Aβ42 and Aβ43 are produced by the second cleavage step of each product line. Like Aβ40 and Aβ38, the CSF concentrations of Aβ42 and Aβ43 are also proportional to each other in controls and in MCI/AD patients [Fig. 12B; ln(Aβ43)=1.333 x ln(Aβ42)-4.09, R=0.979]. On the other hand, the levels of Aβ43 and Aβ40 (a precursor and its product) were correlated in control [Fig. 13A; ln(Aβ43)=0.884 x ln(Aβ40)-4.118, R=0.688] and in MCI/AD subjects (R=0.507/0.736 for MCI/AD, respectively) but the MCI/AD values were located below the regression line for controls and thus provided lower Aβ43 measures compared with controls for a given Aβ40 measure (Fig. 13A; $P<0.001$, ANOVA). Conversely, for a given Aβ43 measure, the plot provided a higher Aβ40 measure in MCI/AD cases. There was a similar situation for the levels of Aβ42 and Aβ38. The levels of Aβ42 and Aβ38 were correlated each other in control subjects [Fig. 13B; ln(Aβ42)=0.724 x ln(Aβ38)+0.251, R=0.723], but barely in MCI/AD (R=0.500 for MCI; 0.393 for AD), and the MCI/AD plots were situated below the regression line for controls ($P<0.001$, ANOVA). For a given Aβ42 measure, the plot provided a higher Aβ38 measure in MCI/AD compared with controls.

These lower concentrations of Aβ42 appeared to be compensated with higher

concentrations of Aβ38 as the levels of ln(Aβ38+Aβ42) did not vary even in MCI/AD (P=0.293, ANOVA). Thus, this points to the possibility that more Aβ42 and Aβ43 are converted to Aβ38 and Aβ40, respectively, in MCI/AD brains. According to numerical simulation based on the stepwise processing model, as the levels of βCTF decline to null, the levels of Aβ43 and 42 decrease and the ratios of Aβ40/43 and Aβ38/42 increase (unpublished data). However, this situation can be excluded as the mechanism for lower concentrations of Aβ42 and 43, because the levels of βCTF have never been reported to be reduced in AD brains nor in plaque-forming Tg2576 mice that show lower CSF Aβ42 concentrations (Kawarabayashi et al, 2001). Thus, it is reasonable to suspect that the final cleavage steps from Aβ43 mostly to 40 and from Aβ42 to 38 are significantly enhanced in parallel (increases in released tri- and tetrapeptides) in brains affected by MCI/AD compared with controls (Fig. 11).

The relationship among γ-secretase-mediated cleavage becomes clearer by plotting the product/precursor ratio representing cleavage efficiency at the step from Aβ42 to 38 (Aβ38/42) against that representing the cleavage efficiency at the step from Aβ43 to 40 (Aβ40/43) (Fig. 14). The "apparent" cleavage efficiency of Aβ43 was approximately 40-fold larger than that of Aβ42. The two ratios in CSF samples from

MCI/AD and control subjects were largely proportional to each other, indicating that the corresponding cleavage processes in the two lines are tightly coupled (Fig. 14). All plots were situated on a distinct line [ln(Aβ38/42)=0.748 x ln(Aβ40/43)-2.244, R=0.936] and its close surroundings. An increase in the cleavage from Aβ43 to 40 (i.e., more Aβ43 is converted to Aβ40) accompanied an increase in the cleavage from Aβ42 to 38 and vice versa, although the mechanism underlying this coupling between the two product lines remains unknown. This reminds me of the "NSAID effect" in the CHAPSO-reconstituted γ-secretase system (Weggen et al, 2001; Takami et al, 2009) in which the addition of sulindac sulfide to the γ-secretase reaction mixture, as expected, significantly suppressed Aβ42 production and increased Aβ38 production presumably by increasing the amounts of released tetrapeptide (VVIA) (Takami et al, 2009) and other peptides.

Most importantly, this graph provides a clear distinction between the control and MCI/AD groups (Fig. 14; Aβ40/43 for MCI/AD vs control, *P*=0.000; Aβ38/42 for MCI/AD vs control, *P*=0.000; ANOVA, followed by Dunnett's t-test). The control measures plotted close to the origin, whereas those for MCI/AD patients were distant from the origin along the line [ln(Aβ38/42)=0.748 x ln(Aβ40/43)-2.244, R=0.936]. It

is also of note that there was no significant difference between MCI and AD patients (Fig. 14; Aβ40/43 for AD vs MCI, *P*=1.000; Aβ38/42 for AD vs MCI, *P*=1.000; Bonferroni's t-test). Two control measures were a little farther from the origin, which may suggest that these subjects already have latent Aβ deposition or are in the preclinical AD stage. Additionally, I examined quite a small number of CSF samples from presenilin (PS) 1-mutated (symptomatic) familial AD (FAD) patients (T116N, L173F, G209R, L286V, and L381V). Out of the three FAD cases near the regression line, two (T116N and L286V) were distant from the origin like sporadic AD cases and one (L381V) was closer to the origin than controls (both Aβ42/43 levels were lower than control; unpublished data). The remaining two (G209R and L173F) were extremely displaced from the line. Thus, a larger number of FAD cases are needed to offer an appropriate explanation for their unusual characteristics in the plot, and the alteration of CSF Aβs shown above seems to be applicable only for sporadic AD.

Altogether, in MCI/AD, more Aβ42 and 43 are processed to Aβ38 and 40, respectively, than in controls. Even in MCI/AD, strict relationships are maintained between the levels of Aβ42 and Aβ43, and between those of Aβ38 and Aβ40 as seen in controls, which are predicted by the stepwise processing kinetics (unpublished

observation). Thus, my observations suggest that lower CSF concentrations of Aβ42 and 43 and presumably higher CSF concentrations of Aβ38 and 40 are the consequence of altered γ-secretase activity in brain rather than the effect of preferential deposition of the two longer Aβ species (Aβ42 and 43) in senile plaques, which would not have maintained such strict relationships between the four Aβ species in CSF.

Measurement of raft-associated γ-secretase activity in human brains-To further test activated γ-secretase hypothesis, I directly measured γ-secretase activities associated with lipid rafts isolated from AD, MCI, and control cortices (Brodmann areas 9-11), because the γ-secretase is thought to be concentrated in rafts (Wada et al, 2003; Hur et al, 2008). All brains cortices were from the Brain Bank at Tokyo Metropolitan Institute of Gerontology (see materials and methods). Rafts were prepared from AD, MCI and control brains, which were frozen within 12h postmortem, as previously described (Oshima et al, 2001; Wada et al, 2003) with some modifications (see materials and methods). Each prepared human brain raft-associated γ-secretase was incubated with purified C99-FLAG *in vitro*, but not long Aβ, to evaluate both Aβ production lines of γ-secretase activity. For definite confirmation of the Aβ species, the reaction mixtures were subjected to quantitative Western blotting

using specific antibodies rather than ELISA. At time 0, deposited Aβ42/43 species were detected in rafts from MCI/AD brains but not in control specimen (Fig. 15). The amounts of ln(Aβ38+Aβ42), which almost reflect the total capacity of the Aβ38/42-producing line, did not vary between AD, MCI and controls (Fig. 16; *P*=0.969, ANOVA). Thus, the gross activities of raft γ-secretase were comparable among the three groups. However, the plots for Aβ40/43 vs Aβ38/42 are divided into two groups: MCI/AD and controls (Fig. 17; Aβ40/43 for control vs MCI/AD, *P*<0.001; Aβ38/42 for control vs MCI/AD, *P*=0.001; Welch's t-test) in the same way as those derived from CSF (Fig. 14). However, ε4-carrying control and MCI/AD subjects did not significantly differ in the γ-secretase activity from other allele-carrying subjects (data not shown). It is notable that Fig. 14 and 17 are based on different methods, ELISA and Western blotting, respectively, but give similar results. There were no significant differences between MCI and AD specimen, although MCI patients (91+/-4.9 year old) were older than controls (77+/-6.5 year old) or AD patients (80+/-5.0 year old) (Aβ40/43 for MCI vs AD, *P*=0.342; Aβ38/42 for MCI vs AD, *P*=0.911). There were similar significant differences between control vs AD in the groups of which the ages were not significantly different (Aβ40/43 for control vs AD,

$P<0.001$; Aβ38/42 for control vs AD, $P=0.03$).

Discussion

γ-Secretase cleaves type I membrane proteins within their transmembrane domains (De Strooper, 2003). The type I membrane proteins as the substrates of γ-secretase are characterized by ectodomain shedding, which is mediated by a wide variety of membrane-bound proteases (sheddases) (De Strooper, 2005). Relationship between ectodomain shedding and intramembrane proteolysis is well-known for the processing of APP, in which ectodomain shedding occurs through α- or β-cleavage (Selkoe, 2001). The cleavages at the α- and β-sites are necessary and sufficient for the execution of γ-cleavage, which results in Aβ production. However, the relationship between γ- and ε-cleavages has remained unclear (Wiley et al, 2005). Although several reports implied that γ- and ε-cleavages are independent processes (Chen et al, 2002; Moehlmann et al, 2002; Hecimovic et al, 2004; Jankowsky et al, 2004), my colleagues previously found that there is a significant correlation between γ- and ε-cleavages (Sato et al, 2003; Funamoto et al, 2004). Here, I have further examined the relationship by taking the advantage of a solubilized γ-secretase assay system with high specific activity, in which use of recombinant C99-FLAG substrate allowed me to exclude contamination by C83-derived AICD. Thus, there are findings using this CHAPSO-solubilized

reconstitution assay system, one is that equal amounts of Aβ and AICD are produced from C99 and that only two species AICD49-99-FLAG and AICD50-99-FLAG are detectable. Another finding is that CHAPSO-solubilized γ-secretase has unusual enzymatic characteristics and these have been shown in case of mtAPP and mtPS1/2. Because of these reasons, Takami et al had shown the 'stepwise processing model' using this established CHAPSO-slubilized γ-secretase assay (Takami et al, 2009).

In this thesis, I assume that i) Aβs in CSF are produced exclusively by γ-secretase in the brain, possibly in neurons; and ii) Aβs in CSF are in the steady state. With these assumptions, the combined measurement of four Aβ species in CSF should predict the activity of γ-secretase in the brain. Here, the alterations in the γ-secretase activities do not mean the gross activity, i.e. total Aβ production, but the cleavage efficiency of the intermediates, Aβ42 and Aβ43.

In the present study, I quantified in CSF the four Aβ species, Aβ38/42 and Aβ40/43, but the Western blotting indicated the presence of additional Aβ species, Aβ37 and 39, in CSF (Fig. 10). At present, I cannot exclude the possibility that a certain carboxyl terminus-specific protease(s) in CSF acts on the pre-existing Aβ species and converts them to Aβ37 and 39 (Zou et al, 2007). However, according to

my unpublished data (Takami et al, unpublished observations), it is plausible that Aβ37 is derived from Aβ40, whereas Aβ39 is derived from Aβ42. Even if so, these pathways are very minor (~20-100-fold less) compared to the two major pathways, Aβ42 to Aβ38, and Aβ43 to Aβ40, when assessed by a CHAPSO-solubilized reconstituted assay system (Takami et al, 2009). Thus, such strict relationships between four Aβs may have been relatively independent of Aβ37 and 39. The detailed relationship between all Aβs in the CSF awaits further quantification of the additional two Aβ species.

Currently, I do not know why the observation that Aβ40 is higher in MCI/AD CSF has so far not been reported except a recent paper (Simonsen et al, 2007). In fact, some of my collaborators previously reported no significant differences in CSF Aβ40 levels between AD and control subjects using a different ELISA (Shoji et al, 1998). It may be notable that I used newly constructed ELISA for Aβ40 based on a different set of monoclonal antibodies and thus, those discrepancies may come from the different antibody/epitope combination and/or different assay methods. In particular, it should be noted that all ELISAs used here detect Aβ1-x only, but not amino-terminally truncated forms. In this context, the ratio of Aβ40/43 appears to be more informative to

discriminate between control and MCI/AD than the absolute levels of Aβ40 alone (Table 3 and Fig. 17). It is possible that even if Aβ40 is not different between control and MCI/AD, the ratio Aβ40/43 could discriminate them.

I am the first to measure CSF Aβ43 using ELISA. The CSF concentrations of Aβ43 are ten-fold less than those of Aβ42. Nevertheless, the specificity of the newly constructed ELISA made the quantification of accurate levels of Aβ43 possible (Fig. 9). Regarding the Aβ43 measures, I observed that its behavior is entirely similar to that of Aβ42 in MCI/AD. My preliminary observations using immunocytochemistry and ELISA quantification strongly suggest that Aβ43 deposits in aged human brains at the same time as Aβ42 (unpublished observations). Furthermore, Saido and colleagues have only recently reported that a PS1 R278I mutation in mice (heterozygous) caused an elevation of Aβ43 and its early and pronounced accumulation in the brain (Saito et al, 2011). It is possible that the cleavage of βCTF by this R278I γ-secretase may be profoundly suppressed in the third cleavage step of the product line 1 (see Fig. 11), which would result in negligible levels of Aβ40 and unusually high levels of Aβ43 (Nakaya et al, 2005). These results suggest that the role of Aβ43 should be reconsidered for the initiation of β-amyloid deposition and thus in the AD

pathogenesis.

The ε4 allele is well known as the strong risk factor for AD. Because the risk increases 3-fold for heterozygous carriers, and even 15-fold for ε4 homozygotes, compared with ε3 homozygotes (Ashford, 2004). This dose dependent manner of the ε4 allele effect also caused a decrease in the AD onset age 84 to 68 years (Coder et al, 1993). However, hetero- and homozygote of ε4 allele subjects did not significantly differ in the CSF Aβ concentrations and raft-associated γ-secretase activity from ε3/ε3-carrying control and MCI/AD subjects (data not shown).

Previous studies focused especially on Aβ42. However lower CSF concentration of Aβ42 is not exclusively limited to MCI/AD. For example, idiopathic normal pressure hydrocephalus (iNPH) has showed not only low concentrations of CSF Aβ42 but also Aβ deposition in brain similar to AD (Silverberg et al, 2003). This raises the possibility that AD and iNPH have a common patho-physiological basis in the CSF circulatory dysfunction. In fact, Aβ42 and 43 were found significantly low in the CSF from eight patients with iNPH (Aβ42, 76.3+/-37.3 pM, P=0.012 compared to controls: Aβ43, 5.2+/-2.9 pM, n=8, P=0.004 compared to controls: Bonferroni's t-test; Silverberg et al, 2003). Thus, lower CSF concentrations of Aβ42 and 43 alone were

unable to distinguish between iNPH and MCI/AD, and further, it is claimed that the former is often associated with abundant senile plaques, raising the possibility that Aβ deposition is enhanced by iNPH (Silverberg et al, 2003). However, when their partners Aβ38 and 40 were measured in CSF, both were found not to be significantly increased in iNPH (Aβ38, 459.2+/-138.5 pM, *P*=0.484 compared to controls; Aβ40, 1094.4+/-375.3 pM, n=8, *P*=0.103 compared to controls; Table 3) in sharp contrast to MCI/AD indicating that the cleavage in iNPH at the steps from Aβ43 to 40 and from Aβ42 to 38 is not enhanced as it is in MCI/AD. Thus, it may be that the dilution effect elicited by ventricular enlargement would be the cause of lower CSF Aβ42 and 43 found in iNPH.

There are a couple of limitations in my thesis. I do not know which comes first Aβ deposition or γ-secretase activity alteration and the mechanism behind the altered activity of brain γ-secretase in MCI/AD (Fig. 14). First, it is of note that rafts prepared from MCI/AD brains but never from control brains at SP stage O/A accumulated Aβ42 and Aβ43 (Fig. 15; Oshima et al, 2001). It is possible that raft-deposited Aβ42/43 could induce a change in the γ-secretase activity, although the extent of the alteration in the activity appears not to be related to the extent of accumulation (unpublished

observation). In this regard, it is of interest to note that Tg2576 mice, the best characterized AD animal model, shows reduced levels of Aβ42 in plasma as well as in CSF at the initial stage of Aβ deposition (Kawarabayashi et al, 2001). If the assumption here is correct, this may suggest that γ-secretase that produces plasma Aβs could also be altered. However, thus far, I have failed to replicate significantly lower Aβ42 levels or Aβ42/Aβ40 ratios in plasma from AD patients.

Second, there could be heterogenous populations of γ-secretase complexes that have distinct activities due to subtle differences in their components. γ-Secretase is a complex of four membrane proteins including PS, nicastrin (NCT), anterior pharynx defective 1 (Aph1) and presenilin enhancer 2 (Pen 2) (Takasugi et al, 2003). Aph 1 has three isoforms, and each can assemble active γ-secretase together with other components (Serneels et al, 2009). Nicastrin, a glycoprotein, is present in immature and mature forms (Yang et al, 2002). The abundance of these heterogenous populations of proteins in the brain is probably under strict control. During MCI/AD, a certain population could replace other populations of γ-secretase and thus may show a distinct activity as a whole.

The data shown here represent only a cross-sectional study, but my keen interest

is how the CSF levels of the four Aβ species would shift during the longitudinal course in an individual who is going to develop sporadic AD. Does one have any period during life when Aβ42 and 43 are at higher levels in CSF, and thus the ratios of Aβ38/42 and Aβ40/43 are smaller? At this period when the final cleavage steps of γ-secretase would be suppressed, the interstitial fluid (ISF) concentrations of Aβ43 and 42 would increase, which would start or promote their aggregation in the brain parenchyma. If so, during life span, the individual's plot would move down along the regression line and move up as senile plaques accumulate, and the individual would eventually develop sporadic AD. However, thus far the period when there are increases in CSF Aβ42/43 has never been reported for sporadic AD. Nor has it been reported for asymptomatic FAD carriers (Ringman et al, 2008), whereas their plasma is known to contain higher levels (and percent) of Aβ42 (Scheuner et al, 1996; Kosaka et al, 1997; Ringman et al, 2008). It is likely that the stage of normal cognition and Aβ accumulation already accompanies reduced CSF Aβ42. If so, the alterations of γ-secretase should continue on for decades. Most interestingly, this alteration of CSF Aβ regulation seems to be planned to prevent further accumulation of Aβ42 and 43 in the brain.

However, Hong et al. (2011) have recently shown, using *in vivo* microdialysis to measure ISF Aβ in APP transgenic mice, that the increasing parenchymal Aβ is closely correlated with decreasing ISF Aβ, suggesting that produced Aβ42 is preferentially incorporated into existing plaque-Aβ. This is a prevailing way of the interpretation of the data. Another way of the interpretation of data would be that during aging from 3 to 24 months, γ-secretase activity becomes altered and produces decreasing amounts of Aβ but with an increasing ratio of Aβ38/42 (and Aβ40/43). It is worth to mention that produced Aβ42 (but not Aβ40) appears to be selectively bound to rafts (from CHO cells) after long incubation (>4h; Wada et al, unpublished observation). Also of note is that I quantified the total (free and bound) Aβ produced by an *in vitro* reconstituted system (Fig. 17). What is claimed here is that decreased levels of CSF Aβ42 are largely due to alterations of γ-secretase activity rather than due to selective deposition of Aβ42 in preexisting plaques. What proportions of decreased ISF (CSF) Aβ42 levels would be contributed to by altered γ-secretase activity and selective deposition of Aβ42/43 to parenchymal plaques awaits future studies.

Finally, my observation has therapeutic implication. As shown elsewhere and here above, if Aβ42 is the culprit for MCI/AD, NSAIDs would have been quite a

reasonable therapeutic compound, which enhances cleavage at the third step in the stepwise processing, leading to lower levels of Aβ42 without greatly interfering with the Aβ bulk flow (Weggen et al, 2001). This sharply contrasts with some of the γ-secretase inhibitors currently under development and in clinical trial, which block the Aβ bulk flow. However, the present study raises the possibility that even if NSAIDs are administered, the expected beneficial effect could be minimal in MCI/AD patients, because in these patient brains, γ-secretase is already shifted to an NSAID-like effect.

Acknowledgment

I am most grateful to Prof. Yasuo Ihara and Dr. Satoru Funamoto, Department of Neuropathology, Factory of Life and Medical Sciences, Doshisha Univ. and Dr. Kazuhiro Nagaike, IBL Co., Ltd. for precise advice and supporting my study, Dr. Takeshi Iwatsubo, Department of Neuropathology, Factory of Medicine, University of Tokyo, for supporting my thesis. I thank Drs. Mikio Shoji, Hiroyuki Arai, Katsutoshi Furukawa and Takeshi Ikeuchi for collection of CSF samples from controls, MCI/AD patients, Drs. Hiroyuki Hatsuta, Shigeo Murayama, Haruyasu Yamaguchi for immunohistochemistry of tissue sections from brains with various Braak senile plaque stages, Drs. Yasuhiro Hashimoto, Masakazu Miyajima, Hajime Arai for collection of CSF samples from iNPH patients, Dr. Kohei Akazawa for statistical analysis, Dr. Ryozo Kuwano for establishment of the appropriate Aβ quantification conditions, Dr. Yu Nagashima for simulation of the stepwise processing model. I also thank all the member of Department of Neuropathology for supporting and encouragement.

References

Adachi T, Saito Y, Hatsuta H, Funabe S, Tokumaru AM, Ishii K, Arai T, Sawabe M, Kanemaru K, Miyashita A, Kuwano R, Nakashima K, Murayama S. Neuropathological asymmetry in argyrophilic grain disease. J Neuropathol Exp Neurol 69:737-744 (2010).

Ashford JW. APOE genotype effects on Alzheimer's disease onset and epidemiology. J Mol Neurosci. 23:157-165 (2004).

Chen F, Gu Y, Hasegawa H, Ruan X, Arawaka S, Fraser P, Westaway D, Mount H, St George-Hyslop P. Presenilin 1 mutations activate gamma 42-secretase but reciprocally inhibit epsilon-secretase cleavage of amyloid precursor protein (APP) and S3-cleavage of notch. J Biol Chem. 277:36521-36526 (2002).

Corder EH, Saunders AM, Strittmatter WJ, Schmechel DE, Gaskell PC, Small GW, Roses AD, Haines JL, Pericak-Vance MA. Gene dose of apolipoprotein E type 4 allele and the risk of Alzheimer's disease in late onset families. Science. 261:921-923 (1993).

De Strooper B. Aph-1, pen-2, and nicastrin with presenilin generate an active gamma-secretase complex. Neuron 38:9-12 (2003).

De Strooper B. Nicastrin: gatekeeper of the gamma-secretase complex. Cell 122:318-320 (2005).

Fraering PC, Ye W, Strub JM, Dolios G, LaVoie MJ, Ostaszewski BL, van Dorsselaer A, Wang R, Selkoe DJ, Wolfe MS. Purification and characterization of the human gamma-secretase complex. Biochemistry. 43:9774-9789 (2004).

Funamoto S, Morishima-Kawashima M, Tanimura Y, Hirotani N, Saido TC, Ihara Y. Truncated carboxyl-terminal fragments of beta-amyloid precursor protein are processed to amyloid beta-proteins 40 and 42. Biochemistry 43:13532-13540 (2004).

Gu Y, Misonou H, Sato T, Dohmae N, Takio K, Ihara Y. Distinct intramembrane cleavage of the beta-amyloid precursor protein family resembling gamma-secretase-like cleavage of Notch. J.Biol. Chem. 276:35235-35238 (2001).

Hayashi I, Urano Y, Fukuda R, Isoo N, Kodama T, Hamakubo T, Tomita T, Iwatsubo T. Selective reconstitution and recovery of functional gamma-secretase complex on budded baculovirus particles. J Biol Chem. 279:38040-38046 (2004).

Hecimovic S, Wang J, Dolios G, Martinez M, Wang R, Goate AM. Mutations in APP have independent effects on Abeta and CTFgamma generation. Neurobiol Dis. 17:205-218 (2004).

Hong S, Quintero-Monzon O, Ostaszewski BL, Podlisny DR, Cavanaugh WT, Yang T, Holtzman DM, Cirrito JR, Selkoe DJ. Dynamic analysis of amyloid β-protein in behaving mice reveals opposing changes in ISF versus parenchymal Aβ during age-related plaque formation. J Neurosci 31:15861-15869 (2011).

Horikoshi Y, Sakaguchi G, Becker AG, Gray AJ, Duff K, Aisen PS, Yamaguchi H, Maeda M, Kinoshita N, Matsuoka Y. Development of Abeta terminal end-specific antibodies and sensitive ELISA for Abeta variant. Biochem Biophys Res Commun. 319:733-737 (2004).

Hur JY, Welander H, Behbahani H, Aoki M, Frånberg J, Winblad B, Frykman S, Tjernberg LO. Active gamma-secretase is localized to detergent-resistant membranes in human brain. FEBS J 275:1174-1187 (2008).

Ishikawa M, Hashimoto M, Kuwana N, Mori E, Miyake H, Wachi A, Takeuchi T, Kazui H, Koyama H. Guidelines for management of idiopathic normal pressure hydrocephalus. Neurol Med Chir (Tokyo) 48 Suppl:S1-23 (2008).

Iwatsubo T, Odaka A, Suzuki N, Mizusawa H, Nukina N, Ihara Y. Visualization of Aβ42(43) and Aβ40 in senile plaque with end-specific Aβ monoclonals: evidence that an initially deposited forms is Aβ42(43). Neuron 13:45-53 (1994).

Jankowsky JL, Fadale DJ, Anderson J, Xu GM, Gonzales V, Jenkins NA, Copeland NG, Lee MK, Younkin LH, Wagner SL, Younkin SG, Borchelt DR. Mutant presenilins specifically elevate the levels of the 42 residue beta-amyloid peptide in vivo: evidence for augmentation of a 42-specific gamma secretase. Hum Mol Genet 13:159-170 (2004).

Kakuda N, Funamoto S, Yagishita S, Takami M, Osawa S, Dohmae N, Ihara Y. Equimolar production of amyloid β-protein and amyloid precursor protein intracellular domain from β-carboxyl-terminal fragment by γ-secretase. J Biol Chem 281:14776-14786 (2006).

Kawarabayashi T, Younkin LH, Saido TC, Shoji M, Ashe KH, Younkin SG. Age-dependent changes in brain, CSF, and plasma amyloid (β) protein in the Tg2576 transgenic mouse model of Alzheimer's disease. J Neurosci 21:372-381 (2001).

Kimberly WT, LaVoie MJ, Ostaszewski BL, Ye W, Wolfe MS, Selkoe DJ. Complex N-linked glycosylated nicastrin associates with active gamma-secretase and undergoes tight cellular regulation. J Biol Chem. 277:35113-35117 (2002).

Kosaka T, Imagawa M, Seki K, Arai H, Sasaki H, Tsuji S, Asami-Odaka A, Fukushima T, Imai K, Iwatsubo T. The βAPP717 Alzheimer mutation increases the percentage of plasma amyloid-beta protein ending at Aβ42(43). Neurology 48:741-745 (1997).

Kuwano R, Miyashita A, Arai H, Asada T, Imagawa M, Shoji M, Higuchi S, Urakami K, Kakita A, Takahashi H, Tsukie T, Toyabe S. Dynamin-binding protein gene on chromosome 10q is associated with late-onset Alzheimer's disease. Hum Mol Genet 15:2170-2182 (2006).

Li G, Aryan M, Silverman JM, Haroutunian V, Perl DP, Birstein S, Lantz M, Marin DB, Mohs RC, Davis KL. The validity of the family history method for identifying Alzheimer disease. Arch Neurol 54:634-640 (1997).

Li YM, Lai MT, Xu M, Huang Q, DiMuzio-Mower J, Sardana MK, Shi XP, Yin KC, Shafer JA, Gardell SJ. Presenilin 1 is linked with gamma-secretase activity in the detergent solubilized state. Proc Natl Acad Sci 97:6138-43 (2000).

Lichtenthaler SF, Wang R, Grimm H, Uljon SN, Masters CL, Beyreuther K. Mechanism of the cleavage specificity of Alzheimer's disease gamma-secretase identified by phenylalanine-scanning mutagenesis of the transmembrane domain of the amyloid precursor protein. Proc Natl Acad Sci 96:3053-3058 (1999).

McKhann G, Drachman D, Folstein M, Katzman R, Price D, Stadlan EM. Clinical diagnosis of Alzheimer's disease: report of the NINCDS-ADRDA Work Group under the auspices of Department of Health and Human Services Task Force on Alzheimer's Disease. Neurology 34:939-944 (1984).

Moehlmann T, Winkler E, Xia X, Edbauer D, Murrell J, Capell A, Kaether C, Zheng H, Ghetti B, Haass C, Steiner H. Presenilin-1 mutations of leucine 166 equally affect the generation of the Notch and APP intracellular domains independent of their effect on Abeta 42 production. Proc Natl Acad Sci 99:8025-8030 (2002).

Nakaya Y, Yamane T, Shiraishi H, Wang HQ, Matsubara E, Sato T, Dolios G, Wang R, De Strooper B, Shoji M, Komano H, Yanagisawa K, Ihara Y, Fraser P, St George-Hyslop, Nishimura M. Random mutagenesis of presenilin-1 identifies novel mutants exclusively generating long amyloid β-peptides. J Biol Chem 280:19070-19077 (2005).

Nyabi O, Pype S, Mercken M, Herreman A, Saftig P, Craessaerts K, Serneels L,

Annaert W, De Strooper B. No endogenous A beta production in presenilin-deficient fibroblasts. Nat Cell Biol 4:164-166 (2002).

Oshima N, Morishima-Kawashima M, Yamaguchi H, Yoshimura M, Sugihara S, Khan K, Games D, Schenk D, Ihara Y. Accumulation of amyloid beta-protein in the low-density membrane domain accurately reflects the extent of beta-amyloid deposition in the brain. Am J Pathol 158: 2209-2218 (2001).

Petersen RC, Doody R, Kurz A, Mohs RC, Morris JC, Rabins PV, Ritchie K, Rossor M, Thal L, Winblad B. Current concepts in mild cognitive impairment. Arch Neurol. 58:1985-1992 (2001).

Pinnix I, Musunuru U, Tun H, Sridharan A, Golde T, Eckman C, Ziani-Cherif C, Onstead L, Sambamurti K. A novel gamma-secretase assay based on detection of the putative C-terminal fragment-gamma of amyloid beta protein precursor. J Biol Chem 276:481-487 (2001).

Qi Y, Morishima-Kawashima M, Sato T, Mitsumori R, Ihara Y. Distinct mechanisms by mutant presenilin 1 and 2 leading to increased intracellular levels of amyloid beta-protein 42 in Chinese hamster ovary cells. Biochemistry 42:1042-1052 (2003).

Qi-Takahara Y, Morishima-Kawashima M, Tanimura Y, Dolios G, Hirotani N, Horikoshi Y, Kametani F, Maeda M, Saido TC, Wang R, Ihara Y. Longer forms of amyloid β protein: Implications for the mechanism of intramembrane cleavage by γ-secretase. J Neurosci 25:436-445 (2005).

Ringman JM, Younkin SG, Pratico D, Seltzer W, Cole GM, Geschwind DH, Rodriguez-Agudelo Y, Schaffer B, Fein J, Sokolow S, Rosario ER, Gylys KG, Varpetian A, Medina LD, Cummings JL. Biochemical markers in persons with preclinical familial Alzheimer disease. Neurology 71:85-92 (2008).

Sato T, Dohmae N, Qi Y, Kakuda N, Misonou H, Mitsumori R, Maruyama H, Koo EH, Haass C, Takio K, Morishima-Kawashima M, Ishiura S, Ihara Y. Potential link between amyloid beta-protein 42 and C-terminal fragment gamma 49-99 of

beta-amyloid precursor protein. J Biol Chem 278:24294-24301 (2003).

Saito T, Suemoto T, Brouwers N, Sleegers K, Funamoto S, Mihira N, Matsuba Y, Yamada K, Nilsson P, Takano J, Nishimura M, Iwata N, Van Broeckhoven C, Ihara Y, Saido TC. Potent amyloidogenicity and pathogenicity of Aβ43. Nat Neurosci 14:1023-1032 (2011).

Scheuner D, Eckman C, Jensen M, Song X, Citron M, Suzuki N, Bird TD, Hardy J, Hutton M, Kukull W, Larson E, Levy-Lahad E, Viitanen M, Peskind E, Poorkaj P, Schellenberg G, Tanzi R, Wasco W, Lannfelt L, Selkoe D, Younkin G. Secreted amyloid β-protein similar to that in the senile plaques of Alzheimer's disease in increase in vivo by the presenilin 1 and 2 and APP mutations linked to familial Alzheimer's disease. Nature Med 2:864-870 (1996).

Schoonenboom NS, Mulder C, Van Kamp GJ, Mehta SP, Scheltens P, Blankenstein MA, Mehta PD. Amyloid β 38, 40, and 42 species in cerebrospinal fluid: more of the same? Ann Neurol 58:139-142 (2005).

Shoji M, Matsubara E, Kanai M, Watanabe M, Nakamura T, Tomidokoro Y, Shizuka M, Wakabayashi K, Igeta Y, Ikeda Y, Mizushima K, Amari M, Ishiguro K, Kawarabayashi T, Harigaya Y, Okamoto K, Hirai S. Combination assay of CSF tau, Aβ1-40 and Aβ1-42(43) as a biochemical marker of Alzheimer's disease. J Neurol Sci 158:134-140 (1998).

Selkoe DJ. Alzheimer's disease: genes, proteins, and therapy. Physiol Rev 81:741-766 (2001).

Serneels L, Van Biervliet J, Craessaerts K, Dejaegere T, Horre K, Van Houtvin T, Esselmann H, Paul S, Schafer MK, Berezovska O, Hyman BT, Sprangers B, Sciot R, Moons L, Jucker M, Yang Z, May PC, Karran E, Wiltfang J, D'Hooge R, De Strooper B. γ-Secretase heterogeneity in the Aph1 subunit: relevance for Alzheimer's disease. Science 324:639-642 (2009).

Shindo N, Nojima S, Fujimura T, Taka H, Mineki R, Murayama K. Separation of 18 6-aminoquinolyl-carbamyl-amino acids by ion-pair chromatography.

Anal Biochem 249:79-82 (1997).

Silverberg GD, Mayo M, Saul T, Rubenstein E, McGuire D. Alzheimer's disease, normal-pressure hydrocephalus, and senescent changes in CSF circulatory physiology: a hypothesis. Lancet Neurol 2:506-511 (2003).

Simonsen AH, Hansson SF, Ruetschi U, McGuire J, Podust VN, Davies HA, Mehta P, Waldemar G, Zetterberg H, Andreasen N, Wallin A, Blennow K. Amyloid β 1-40 quantification in CSF: comparison between chromatographic and immunochemical methods. Dement Geriatr Cogn Disord 23:246-250 (2007).

Takami M and Ihara Y unpublished observations.

Takami M, Nagashima Y, Sano Y, Ishihara S, Morishima-Kawashima M, Funamoto S, Ihara Y (2009) γ-Secretase: Successive tripeptide and tetrapeptide release from the transmembrane domain of β-carboxyl terminal fragment. J Neurosci 29:13042-13052.

Takasugi N, Tomita T, Hayashi I, Tsuruoka M, Niimura M, Takahashi Y, Thinakaran G, Iwatsubo T. The role of presenilin cofactors in the γ-secretase complex. Nature 422:438-441 (2003).

Tian G, Sobotka-Briner CD, Zysk J, Liu X, Birr C, Sylvester MA, Edwards PD, Scott CD, Greenberg BD. Linear non-competitive inhibition of solubilized human gamma-secretase by pepstatin A methylester, L685458, sulfonamides, and benzodiazepines. J Biol Chem 277:31499-31505 (2002).

Tomita S, Kirino Y, Suzuki T. A basic amino acid in the cytoplasmic domain of Alzheimer's beta-amyloid precursor protein (APP) is essential for cleavage of APP at the alpha-site. J Biol Chem 273:19304-19310 (1998).

Tsukie T and Kuwano R unpublished observations.

Wada S and Ihara Y unpublished observations.

Wada S, Morishima-Kawashima M, Qi Y, Misonou H, Shimada Y, Ohno-Iwashita Y,

Ihara Y. Gamma-secretase activity is present in rafts but is not cholesterol-dependent. Biochemistry 47:13977-13986 (2003).

Weggen S, Eriksen JL, Das P, Sagi SA, Wang R, Pietrzik CU, Findlay KA, Smith TE, Murphy MP, Bulter T, Kang DE, Marquez-Sterling Z, Golde TE, Koo EH. A subset of NSAIDs lower amyloidogenic Aβ42 independently of cyclooxygenase activity. Nature 414:212-216 (2001).

Wiley JC, Hudson M, Kanning KC, Schecterson LC, Bothwell M. Familial Alzheimer's disease mutations inhibit gamma-secretase-mediated liberation of beta-amyloid precursor protein carboxy-terminal fragment. J Neurochem 94:1189-1201 (2005).

Winblad B, Palmer K, Kivipelto M, Jelic V, Fratiglioni L, Wahlund LO, Nordberg A, Backman L, Albert M, Almkvist O, Arai H, Basun H, Blennow K, de Leon M, DeCarli C, Erkinjuntti T, Giacobini E, Graff C, Hardy J, Jack C, Jorm A, Ritchie K, van Duijn C, Visser P, Petersen RC. Mild cognitive impairment--beyond controversies, towards a consensus: report of the International Working Group on Mild Cognitive Impairment. J

Intern Med 256:240-246 (2004).

Yagishita S, Morishima-Kawashima M, Tanimura Y, Ishiura S, Ihara Y. DAPT-induced intracellular accumulations of longer amyloid beta-proteins: further implications for the mechanism of intramembrane cleavage by gamma-secretase. Biochemistry 45:3952-3960 (2006).

Yang DS, Tandon A, Chen F, Yu G, Yu H, Arakawa S, Hasegawa H, Duthie M, Schmidt SD, Ramabhadran TV, Nixon RA, Mathews PM, Gandy SE, Mount HT, St Georgy-Hyslop P, Fraser PE. Mature glycosylation and trafficking of nicastrin modulate its binding to presenilins. J Biol Chem 277:28135-28142 (2002).

Zhao G, Cui MZ, Mao G, Dong Y, Tan J, Sun L, Xu X. gamma-Cleavage is dependent on zeta-cleavage during the proteolytic processing of amyloid precursor protein within its transmembrane domain. J Biol Chem 280:37689-37697 (2005).

Zhao G, Mao G, Tan J, Dong Y, Cui MZ, Kim SH, Xu X. Identification of a new presenilin-dependent zeta-cleavage site within the transmembrane domain of amyloid precursor protein. J Biol Chem 279:50647-55060 (2004).

Zou K, Yamaguchi H, Akatsu H, Sakamoto T, Ko M, Mizoguchi K, Gong JS, Yu W, Yamamoto T, Kosaka K, Yanagisawa K, Michikawa M. Angiotensin-converting enzyme converts amyloid β-protein 1-42 (Aβ(1-42)) to Aβ(1-40), and its inhibition enhances brain Aβ deposition. J Neurosci 27:8628-8635 (2007).

Ethics

For all the brains registered at the bank and CSF samples we obtained written informed consents for their use for medical research from patient or patient's family.

同大倫乙 2007 第 46 号　（同志社大学倫理委員会）

同大倫乙 2008 第 61 号　（同志社大学倫理委員会）

承認番号 2008-134（東北大学倫理委員会）

承認番号 2007-109（2012-112 へ継続中）（弘前大学倫理委員会）

承認番号 2007-631（新潟大学倫理委員会）

承認番号 2007-1887（東京大学倫理委員会）

Fig.1

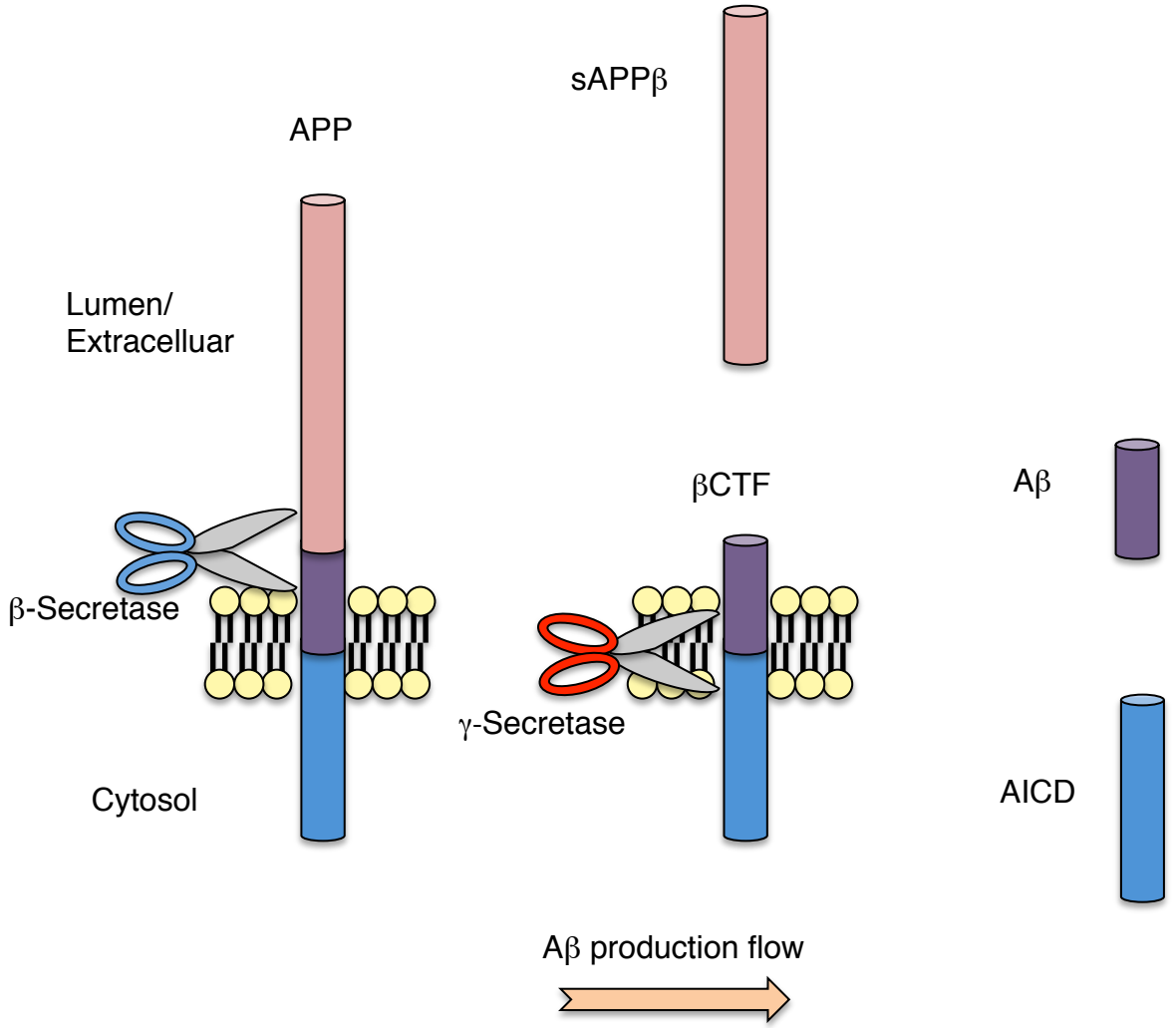

Figure 1. APP processing mechanism for Aβ production. APP is a type-I transmembrane protein. APP is cleaved by β-secretase at lumen portion to generate a βCTF. Soluble APP (sAPPβ) is released from transmembrane. Sequentially, γ-secretase cleaves βCTF in transmembrane to produce each Aβ. Almost Aβ would secreted immediately, and AICD would gone to nuclear.

Fig.2

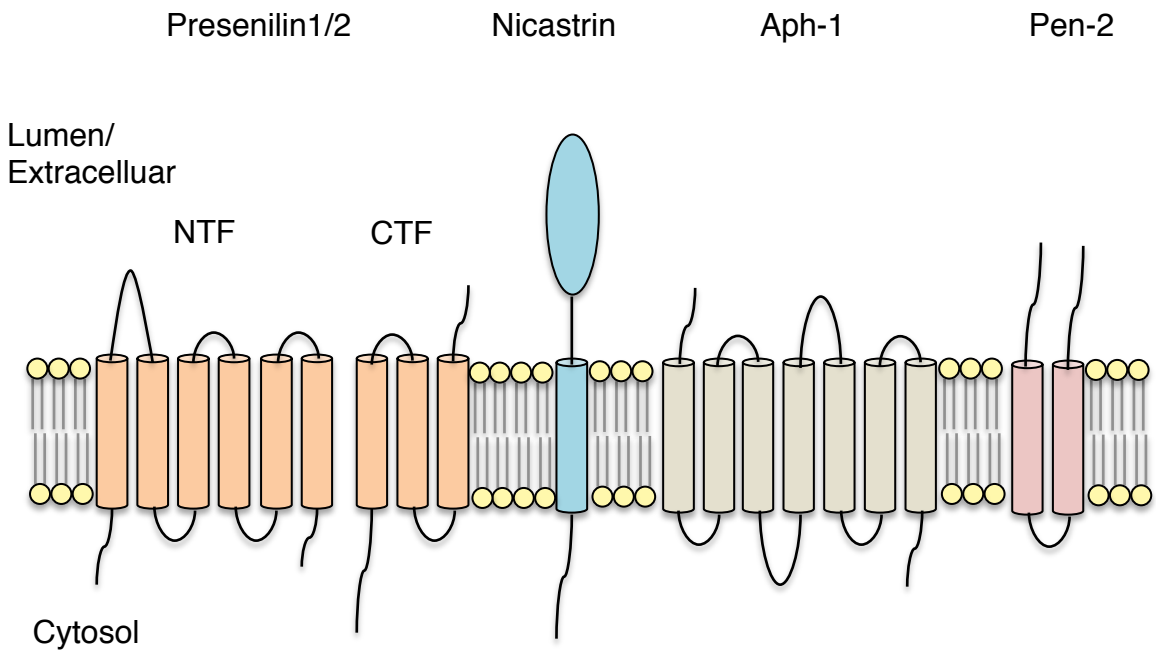

Figure 2. Subunit of the γ-secretase complex and their mambrane topologies. Presenilin 1 or 2 is proteolytically processed into two fragments, an amino-terminal fragmant (NTF) and a carboxyl terminal fragment (CTF). Presenilin 1 or 2 make up the catalytic site of γ-secretase. Other subunits are Nicastrin, Aph-1 and Pen-2.

Fig.3

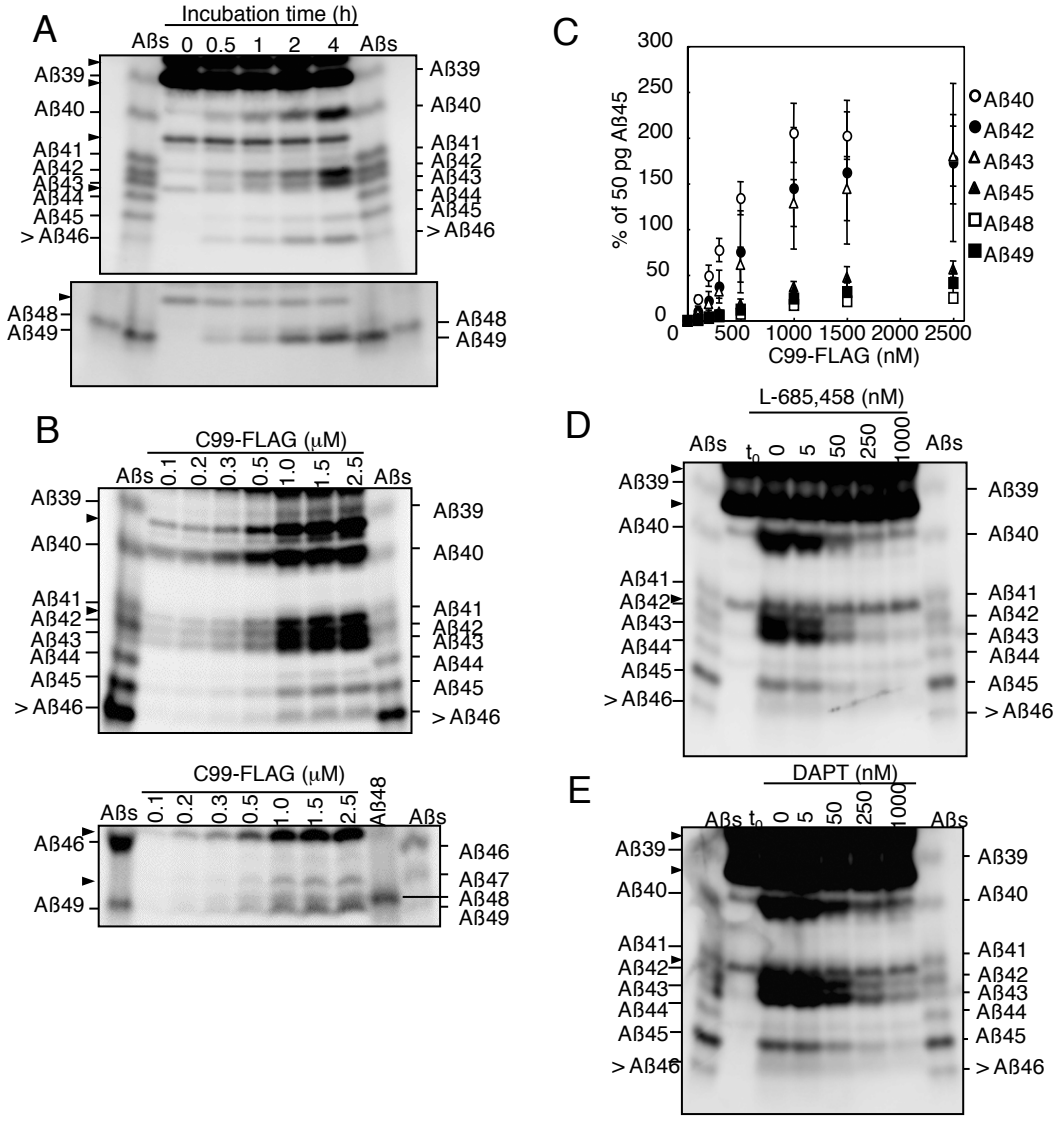

Figure 3. Aβ species generated by the solubilized γ-secretase assay system. A: The microsomal fraction of CHO cells was solubilized with CHAPSO and incubated with 500 nM C99-FLAG; the reaction was terminated at the time indicated by placing a reaction tube on ice. The Aβs produced, together with synthetic authentic Aβs, were separated on gel I (upper panel) and gel II (lower panel), followed by western blotting with 82E1, a monoclonal antibody specific for the N-terminus of Aβ. Aβ40, Aβ42, Aβ43 and Aβ45 were produced in a time-dependent manner. Aβ46 and longer Aβs were stuck at the bottom of gel I. Gel II showed that the longer Aβs were Aβ48 and Aβ49 and that they were also produced in a time-dependent manner. B: Defined amounts of C99-FLAG were incubated with CHAPSO-solubilized microsomal fraction of CHO cells. Protein samples were separated on gel I and II. Against increasing concentrations of C99-FLAG, intensities of each Aβ species were plotted as percentage of 50 pg synthetic Aβ45. Retaining efficiencies of various Aβs were postulated to be the same. C: Data represent means ± SD of three independent experiments. Apparent *K*m and *V*max values are summarized in Table 1. D and E: The CHAPSO-solubilized microsomal fraction was incubated with 500 nM C99-FLAG in the presence of L-685,458 (D) and DAPT (E) at the indicated concentrations. Production of all Aβ species was uniformly suppressed by both γ-secretase inhibitors in a dose-dependent manner. This contrasts with findings in cell-based or cell-free assay systems, in which DAPT induces differential accumulation of Aβ43 and Aβ46. Arrowheads indicate C-terminally truncated, C99-FLAG fragments (Qi-Takahara et al, 2005).

Fig.4

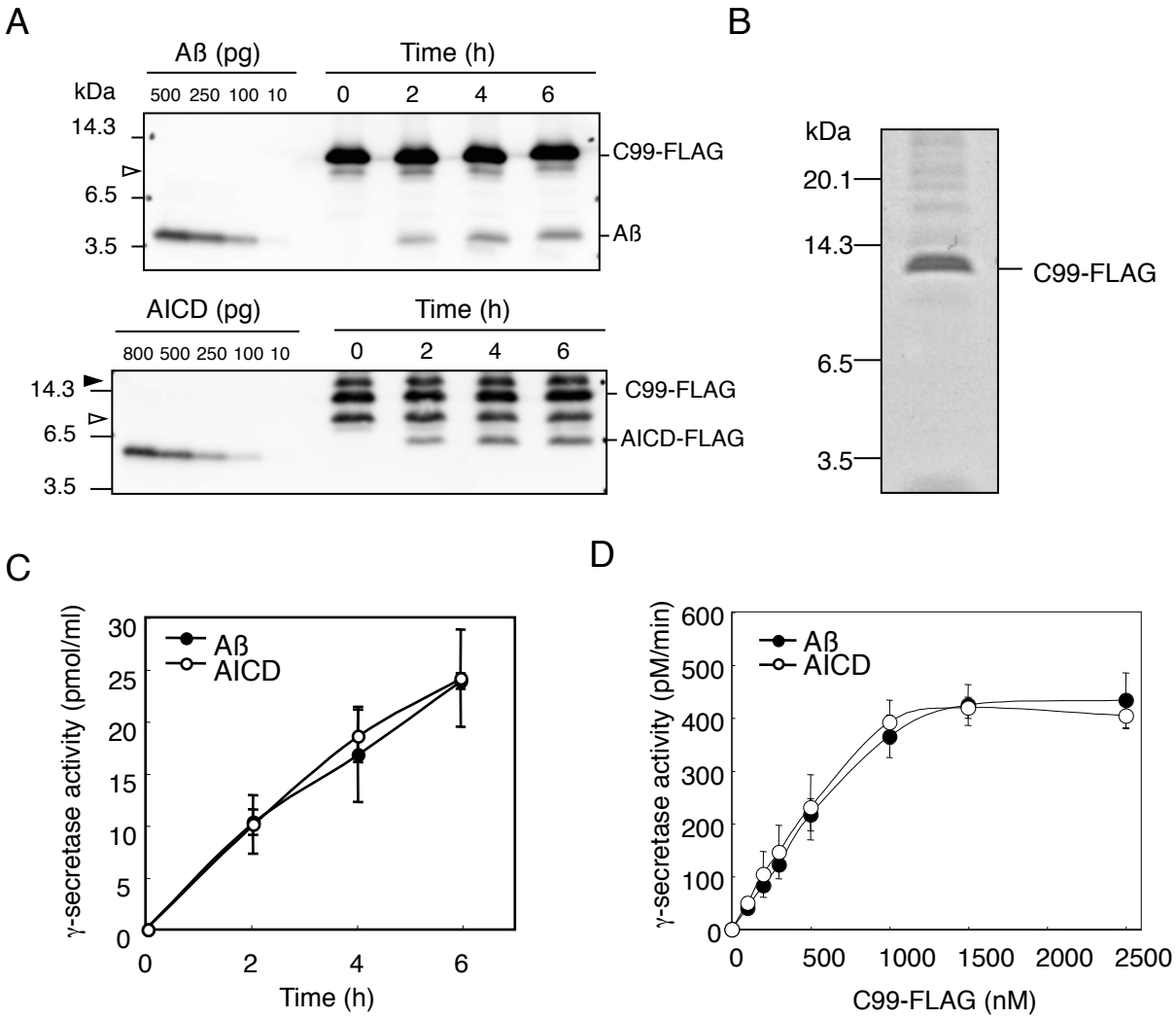

Figure 4. Stoichiometry between Aβ and AICD. The CHAPSO-solubilized microsomal fraction of CHO cells was incubated with 500 nM C99-FLAG, and the reaction was terminated at the time indicated by placing a tube on ice. Aβs were separated on 16.5% gel with defined amounts of synthetic Aβ40 and CTF50-99 as controls for quantification, and subjected to western blotting using 82E1 (A, upper panel) and UT-421 (A, lower panel). The highest-molecular-mass band at about 15 kDa and lowest-molecular-mass band at about 9 kDa, before incubation represent presumably N-terminally extended C99-FLAG with residual signal peptide and truncated C99-FLAG, respectively. CBB staining cannot detect those fragments (B). Equal amounts of Aβ and AICD were produced in a time-dependent manner (C). D: The CHAPSO-solubilized fraction was incubated with varying amounts of C99-FLAG, and produced Aβ and AICD were quantified. The amounts of Aβ and AICD generated after 3 h are plotted against C99-FLAG concentrations. The kinetics of Aβ and AICD was statistically indistinguishable ($p > 0.1$, Student's t-test) and apparently fit the Michaelis-Menten curve. Apparent Km (Kapp) values for Aβ and AICD were almost identical and summarized in Table 2. Closed arrowhead, C99-FLAG with residual signal peptide; open arrowhead, C-terminally truncated C99-FLAG; closed circle, Aβ; open circle, AICD. Values represent means ± SD of three independent experiments.

Fig.5

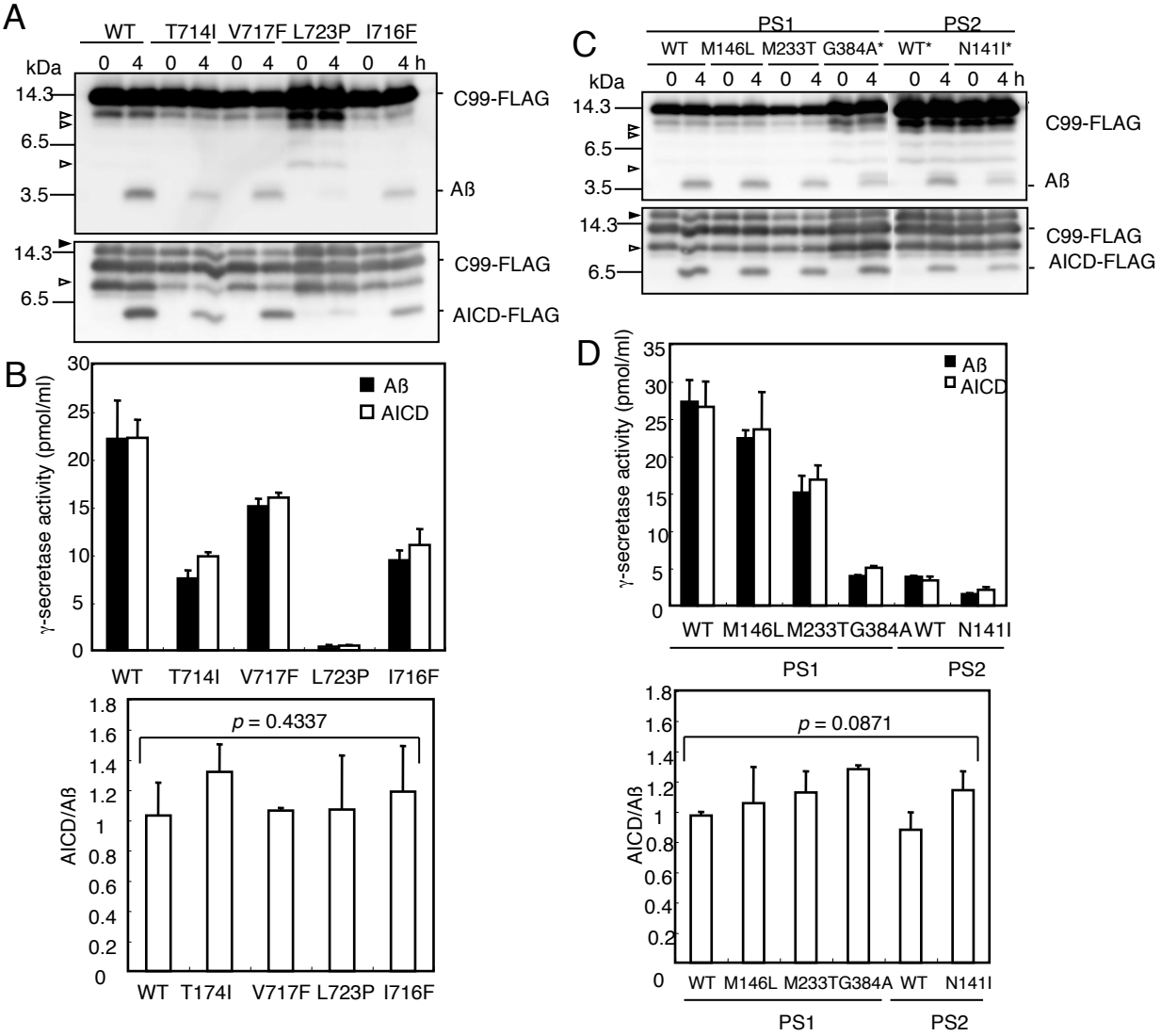

Figure 5. Stoichiometry between Aβ and AICD in mtC99 and mtPS1/2. T714I, V717F, L723P or an artificial mutation I716F (I45F, according to Aβ numbering) was introduced into C99-FLAG. Each mtC99-FLAG at 500 nM was incubated with a CHAPSO-solubilized lysate for three hours. A: Reaction mixtures were subjected to western blotting for Aβ (upper panel) and AICD (lower panel) using 82E1 and UT-421, respectively. Bands indicated by closed and open arrowheads were presumably C99-FLAG with residual signal peptide and C-terminally truncated C99-FLAG, respectively. B: Quantification of Aβ and AICD produced from C99-FLAG is shown in the left panel. MtC99-FLAGs produced significantly reduced amounts of Aβ and AICD, but showed no statistically significant alteration in their stoichiometry (Kruskal-Wallis test) (B, lower panel). C: CHAPSO-solubilized lysate of CHO cells expressing mtPS1/2 was incubated with wtC99-FLAG. Aβ (upper panel) and AICD (lower panel) production was quantified for each wt or mtPS1/2 (D, upper panel). In G384A mtPS1, an additional band, which was included for the quantification of Aβ, was detected above the Aß band and identified as a mixture of Aß48 and Aβ49 (data not shown). As found, mtPS1/2 produced reduced amounts of Aβ and AICD, but both were equivalently generated (lower panel). The stoichiometry between Aβ and AICD was not altered across various C99s and PS1/2s (Kruskal-Wallis test). Asterisks in C indicate the samples for which four-fold more than other samples was loaded onto the gel. Closed arrowhead, C99-FLAG with signal peptide; open arrowhead, truncated C99-FLAG; closed bar, Aβ; and open bar, AICD. Values represent means ± SD of three independent experiments.

Fig.6

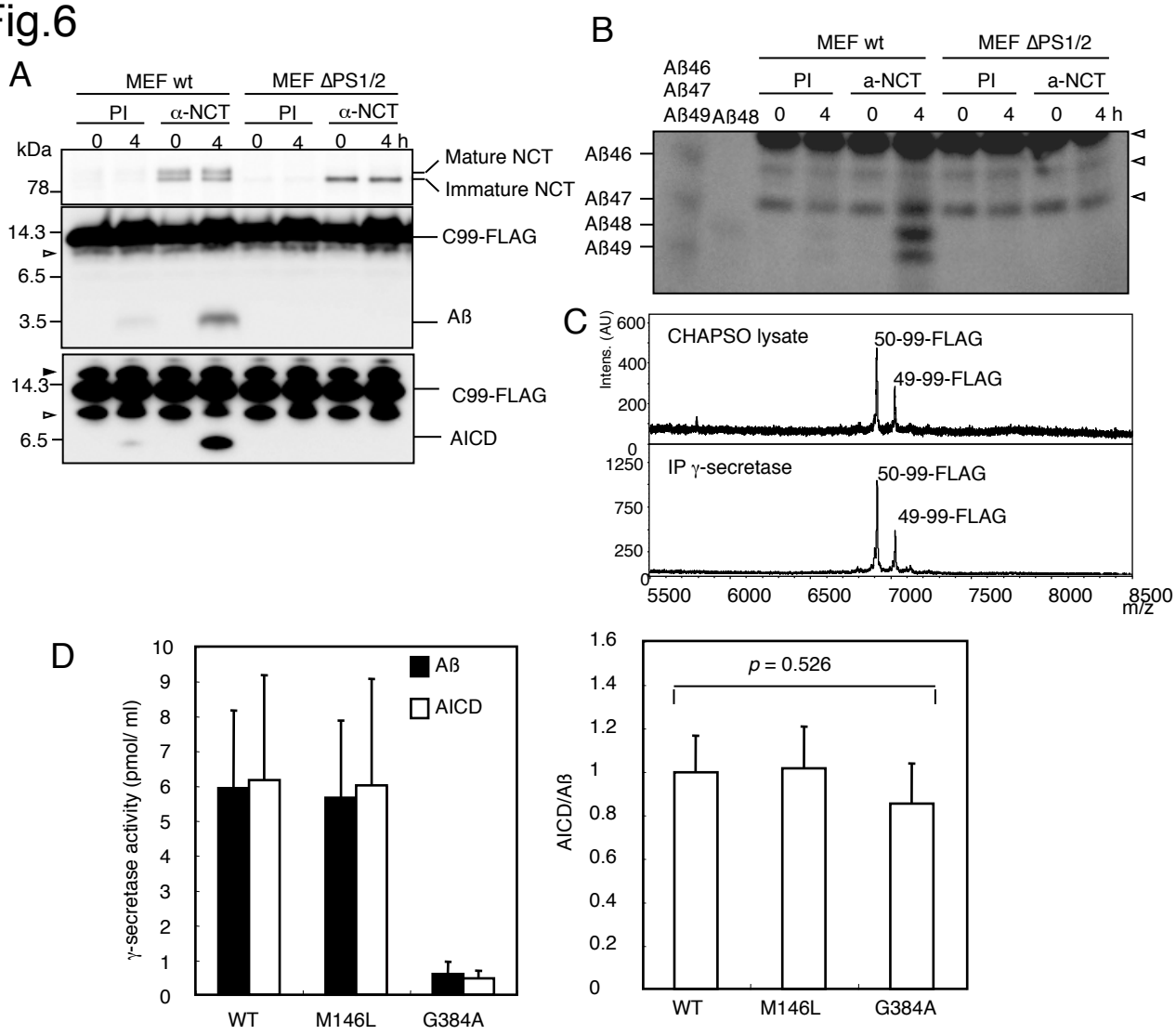

Figure 6. γ-Secretase complex was immunoprecipitated with anti-nicastrin antibody from MEF lysate and was incubated with C99-FLAG. A: Visualization by anti-nicastrin antibody indicates that the immunoprecipitate from wtMEF contained mature nicastrin, while that from PS1/2-deficient MEF contained only immature nicastrin (upper panel). The γ-secretase complex from wtMEF produced Aβ and AICD in the presence of C99-FLAG (middle and lower panels). In contrast, the immunoprecipitates with preimmune serum (PI) generated negligible amounts of Aβ and AICD in the presence of C99-FLAG. No product was generated with the immunoprecipitate from PS1/2-deficient MEF. Importantly, Aβ48 and Aβ49 were detectable only in case of the immunoprecipitate from wtMEF (B). AICDs generated in CHAPSO-solubilized lysate and with partially purified γ-secretase complex were immunoprecipitated with FLAG antibody and subjected to TOF mass spectrometry. As found in cell-free assay, only AICD49-99-FLAG and AICD50-99-FLAG were detected in either case (C). D: Equimolar production of Aβ and AICD from C99-FLAG with partially purified γ-secretase complex. γ-Secretase was immunoprecipitated from lysate of CHO cells expressing wtPS1 or mtPS1 and incubated with C99-FLAG. Reaction mixtures were subjected to quantitative western blotting with defined amounts of Aβ40 and purified AICD50-99-FLAG as controls. G384A mtPS1 exhibited significant reduction of Aβ and AICD, as observed in the CHAPSO lysate (left panel). Equal amounts of Aβ and AICD were produced, irrespective of PS1 mutations (right panel). Closed arrowhead, C99-FLAG with signal peptide; open arrowhead, C-terminally truncated C99-FLAG. Values represent means ± SD of three independent experiments.

Fig.7

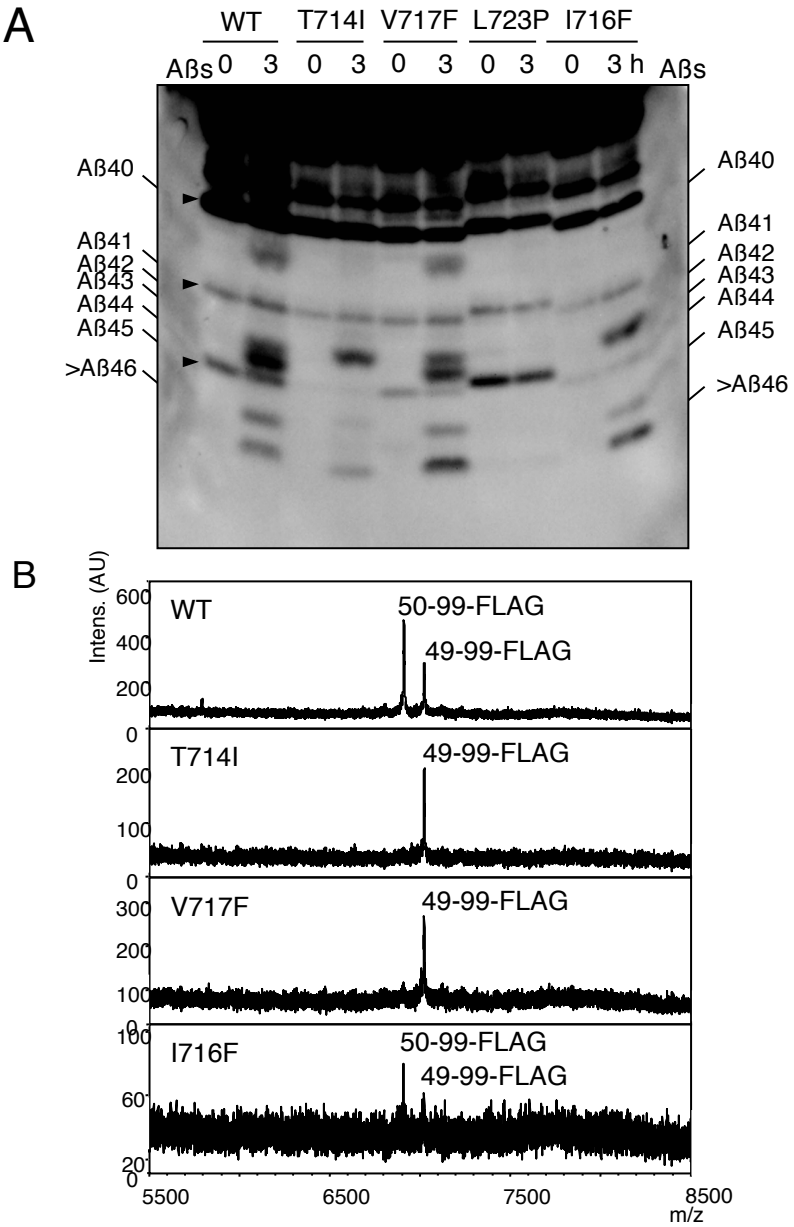

Figure 7. Aβ (A) and AICD (B) species generated from wt or mtC99-FLAG. A: Each wt or mtC99-FLAG at 500 nM was incubated with a CHAPSO-solubilized lysate of CHO cells, and the reaction mixture was subjected to gel system I. In wtC99-FLAG, robust signals for Aβ42 and Aβ43 as well as Aβ40 were detected on the blot. V717F mutation resulted in similar proportions of Aβ species. In contrast, T714I and I716F mutations led to predominant production of Aβ42. L723P mutation generated neither Aβ nor AICD in our hands. Arrowheads indicate C-terminally truncated C99-FLAG fragments. B: The generated AICD species were immunoprecipitated and subjected to TOF mass spectrometry. AICD50-99-FLAG and AICD49-99-FLAG were identified from a wtC99-FLAG-containing reaction mixture with the former signal being stronger. Interestingly, only AICD49-99-FLAG was detected from the reaction mixtures containing T714I and V717F mtC99-FLAG. In artificial mutant I716F, both AICD50-99-FLAG and AICD49-99-FLAG were identified despite predominant production of Aß42. These indicate that FAD mutations downstream of the γ-cleavage sites cause significant alterations in the ε-cleavage sites.

Fig.8

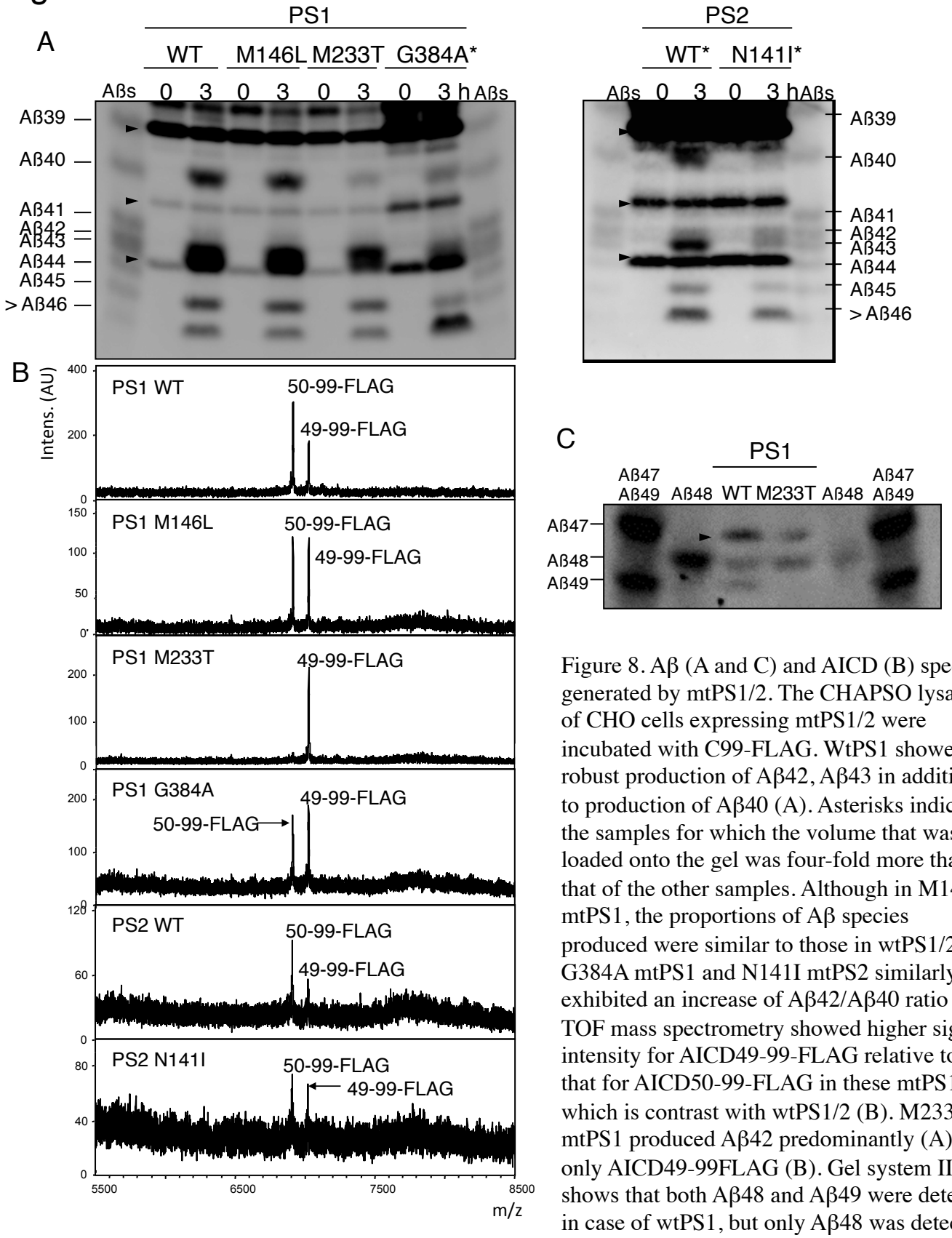

Figure 8. Aβ (A and C) and AICD (B) species generated by mtPS1/2. The CHAPSO lysates of CHO cells expressing mtPS1/2 were incubated with C99-FLAG. WtPS1 showed robust production of Aβ42, Aβ43 in addition to production of Aβ40 (A). Asterisks indicate the samples for which the volume that was loaded onto the gel was four-fold more than that of the other samples. Although in M146L mtPS1, the proportions of Aβ species produced were similar to those in wtPS1/2, G384A mtPS1 and N141I mtPS2 similarly exhibited an increase of Aβ42/Aβ40 ratio (A). TOF mass spectrometry showed higher signal intensity for AICD49-99-FLAG relative to that for AICD50-99-FLAG in these mtPS1/2, which is contrast with wtPS1/2 (B). M233T mtPS1 produced Aβ42 predominantly (A) and only AICD49-99FLAG (B). Gel system II shows that both Aβ48 and Aβ49 were detected in case of wtPS1, but only Aβ48 was detected in M233T mtPS1, probably as a counterpart of AICD49–99-FLAG (C). Arrowheads indicate C-terminally truncated C99-FLAG.

Fig.9

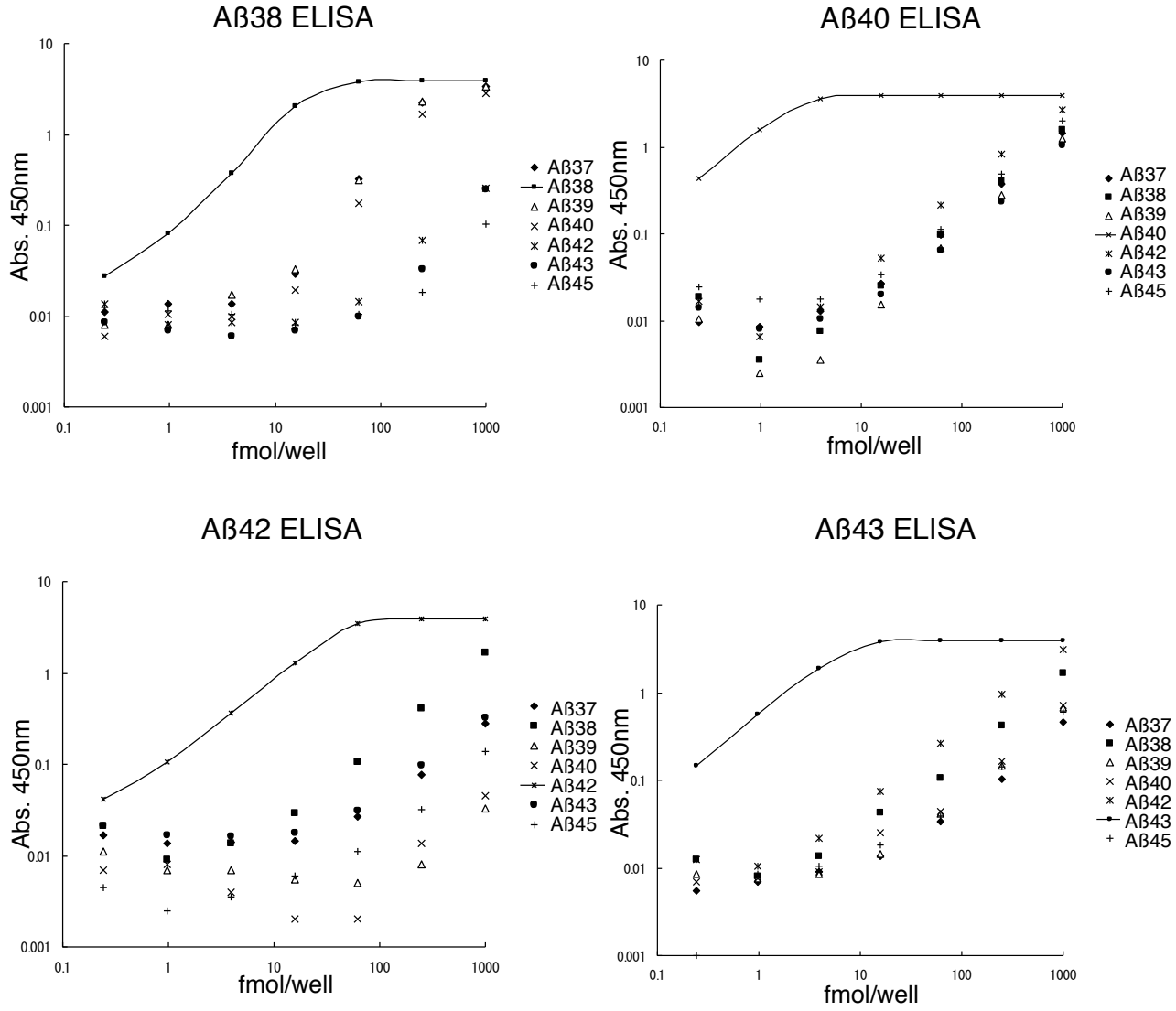

Figure 9. Specificities of the ELISAs: Each amount of Aβ37, Aβ38, Aβ39, Aβ40, Aβ42, Aβ43 or Aβ45 was placed on the plate coated with each carboxyl terminus–specific antibody. HRP-labeled 82E1 (specific for the amino terminus of human Aβ) was used to detect bound Aβ1-x, except Aβ38 ELISA in which 82E1 is used as the capture with Aβ38 carboxyl terminus–specific HRP-labeled antibody as the detector.

Fig.10

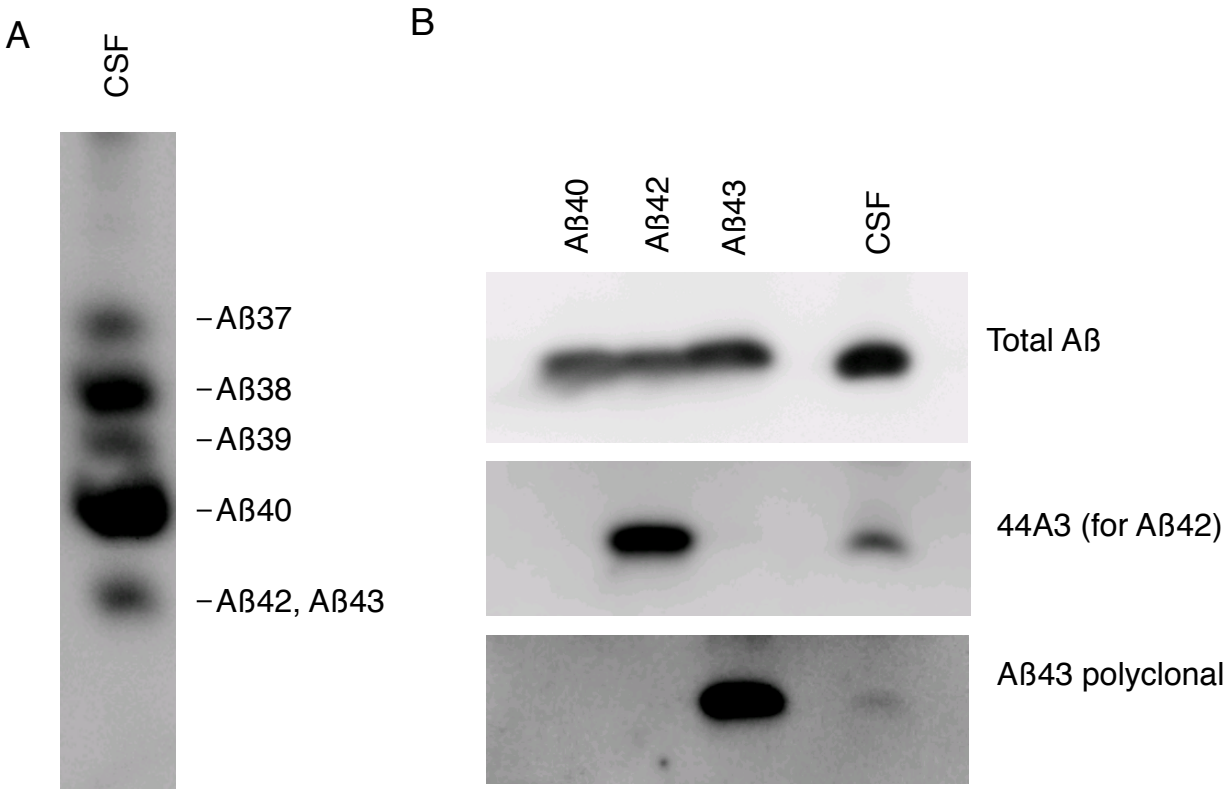

Figure 10. A: The presence of Aβs in CSF, as shown by Western blotting. Aβs in CSF were immunoprecipitated with 82E1. The 82E1-immunoprecipitated Aβs were loaded onto a lane and subjected to Tris/Tricine/8M urea SDSPAGE. After electrotransfer, the blot was immunolabeled with 82E1. Aβ42 and 43 were hardly separated under the conditions.
B: The presence of Aβ42 and Aβ43 in CSF, as shown by Western blotting. One hundred picograms for each authentic Aβ and the 82E1-immunoprecipitate (right-most lane) were loaded onto each lane and subjected to Tris/Tricine SDS–PAGE. After electrotransfer, the blot was immunolabeled with 82E1, 44A3 (specific for Aβ42) or Aβ43 polyclonal antibody.

Fig.11

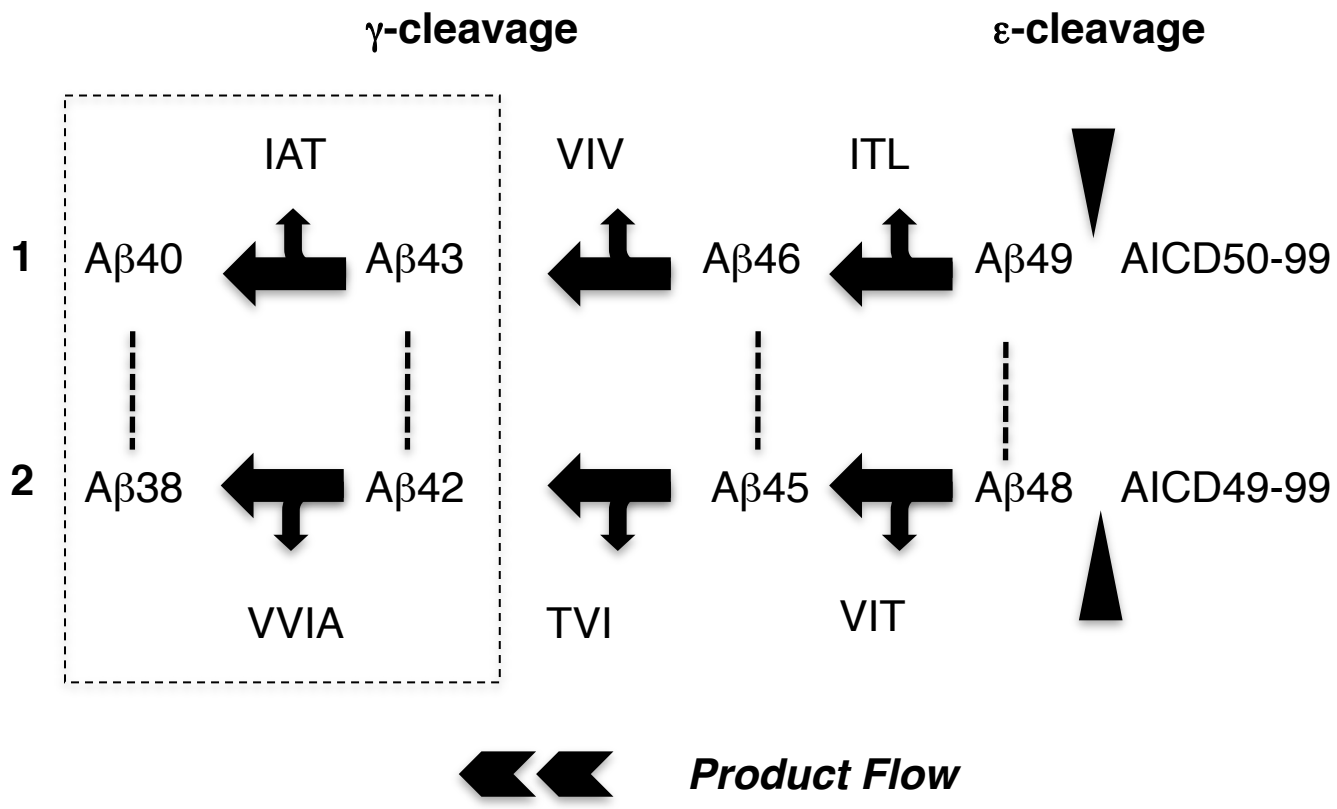

Figure 11. Stepwise processing of βCTF. At the first step, βCTF is cleaved at the membrane-cytoplasmic boundary (ε-cleavage), producing AICD (APP intracellular domain) 50-99 and 49-99. Counterparts Aβ49 and 48 in turn are cleaved in a stepwise fashion, releasing tri- and tetrapeptides. One product line converts Aβ49 mostly to Aβ40 via Aβ46 and Aβ43. The other product line converts Aβ48 to Aβ38 via Aβ45 and Aβ42. It should be noted that the differences between the amounts of released tri- or tetrapeptide determine the amounts of Aβs produced. Broken lines indicate corresponding Aβs on the two product lines.

Fig.12

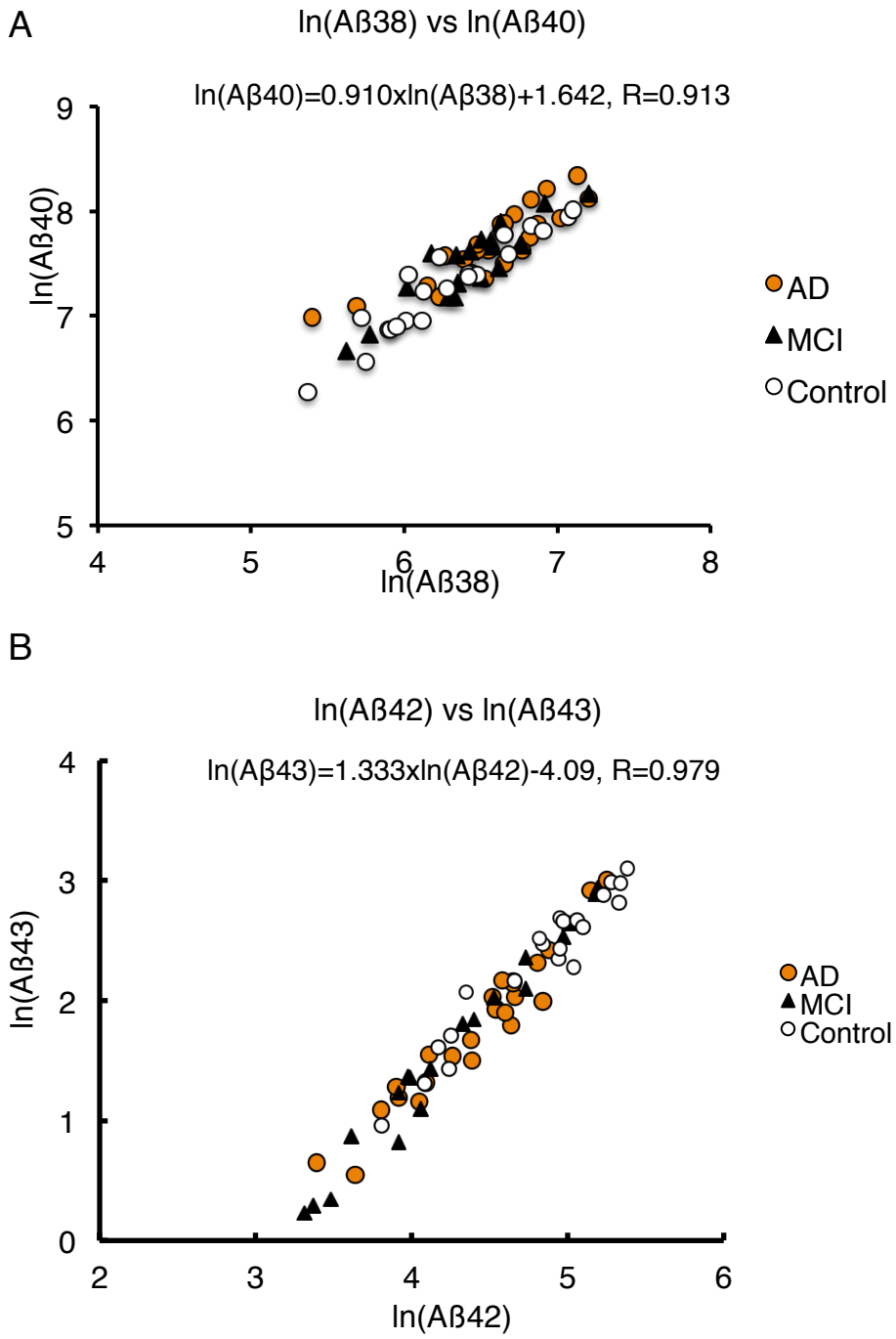

Figure 12. Relationships between the levels of Aβ40 and 38 (A), and between those of Aβ43 and 42 (B) in CSF from controls and MCI/AD patients. All CSF samples were measured by ELISA for Aβ38, 40, 42, and 43. The levels of ln(Aβ40) were proportional to those of ln(Aβ38) (A; ln(Aβ40)=0.910xln(Aβ38)+1.642, R=0.913), while those of ln(Aβ43) were proportional to those of ln(Aβ42) (B; ln(Aβ43)=1.333 x ln(Aβ42)-4.09, R=0.979). It should be noted that the levels of both ln(Aβ42) and ln(Aβ43) in MCI [filled triangle (n=19)]/AD [orange circle (n=24)] are lower than those in controls [open circles (n=21)].

Fig.13

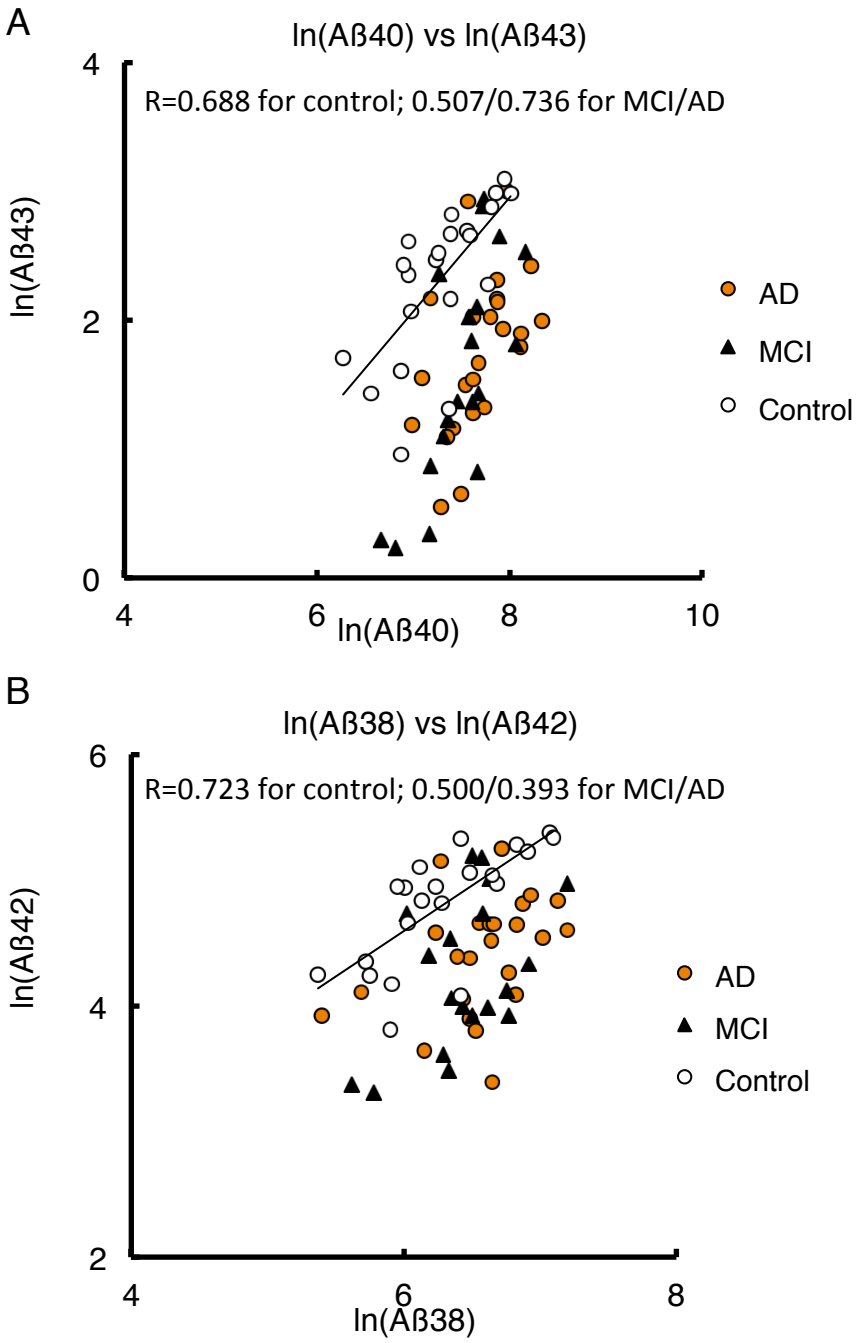

Figure 13. Relationships between the levels of Aβ43 and 40 (A), and between those of Aβ42 and 38 (B) in CSF from controls (open circles) and MCI (closed triangle)/AD patients (orange circle). A: The levels of ln(Aβ43) correlate with those of ln(Aβ40) within controls (R=0.688), and barely within MCI/AD subjects (R=0.507/0.736). The plots for MCI/AD were located below the regression line for control (solid line; *P*<0.001, ANOVA). B: The levels of Aβ42 correlate with those of Aβ38 within controls (R=0.723), and barely within MCI/AD (R=0.500/0.393). The plots for MCI/AD were situated below the regression line for controls (solid line; *P*<0.001, ANOVA).

Fig.14

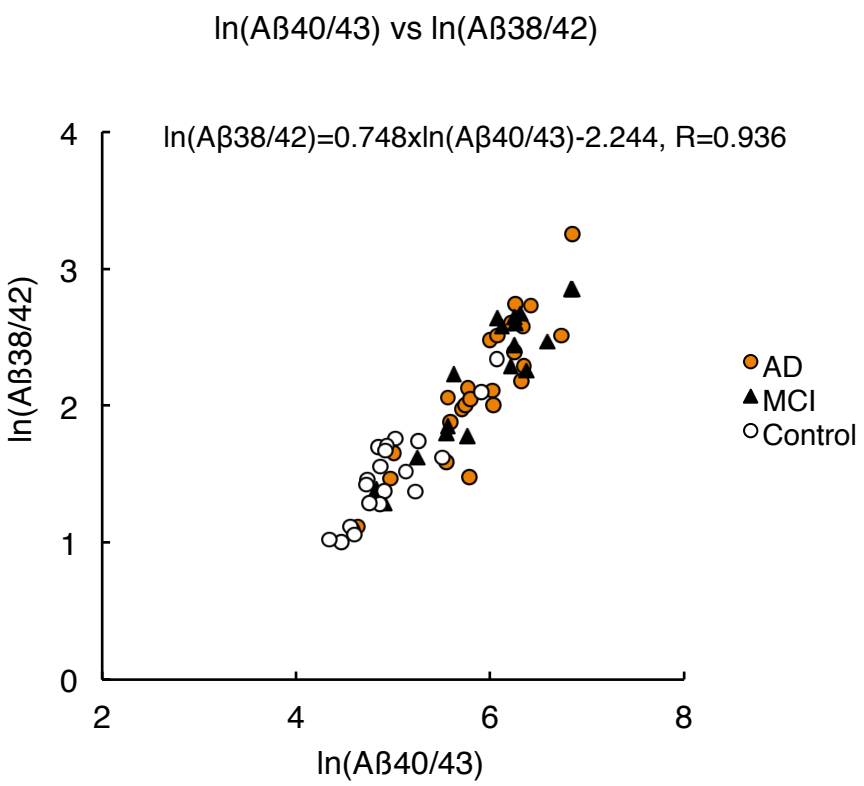

Figure 14. Ln(Aβ40/43) vs ln(Aβ38/42) plot. The ratios represent the cleavage efficiency at the final step of each line. Both ratios are largely proportional to each other (ln(Aβ38/42)=0.748 x ln(Aβ40/43)-2.244, R=0.936) and plots are located on the line and its close surroundings. This plot clearly distinguishes between control subjects and MCI/AD patients (Aβ40/43 for MCI vs control, *P*=0.000; Aβ38/42 for MCI vs control, *P*=0.000; ANOVA, followed by Dunnett's t-test). Control plots [open circles (n=21)] are located close to the origin and MCI/AD plots [closed triangles (n=19) and orange circles (n=24), respectively] are a little distant from the origin.

Fig.15

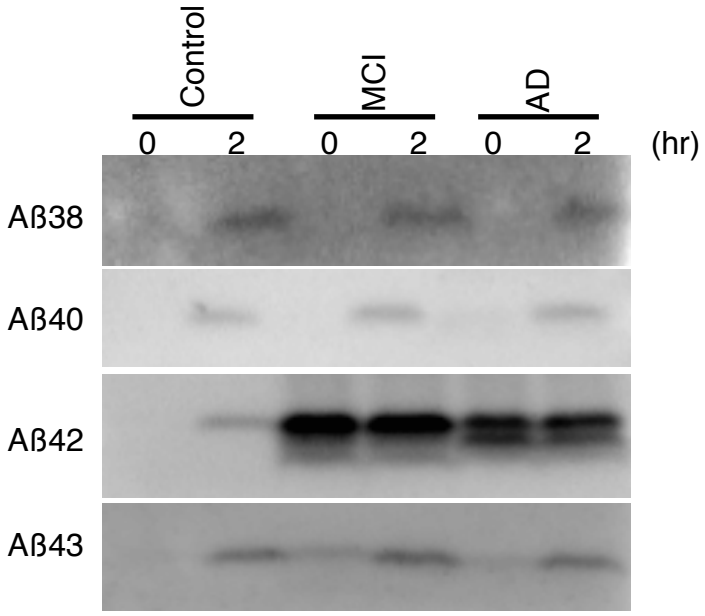

Figure 15. The production of Aβs by raft-associated γ-secretase prepared from control, MCI and AD cortices (Brodmann areas 9-11), as assessed by Western blotting. The samples were loaded onto each lane and subjected to Tris/Tricine SDS–PAGE. After electrotransfer, the blot was immunolabeled with 3B1 (specific for Aβ38), BA27 (specific for Aβ40), 44A3 (specific for Aβ42) and Aβ43 polyclonal antibody. At time 0, MCI/AD specimens accumulated Aβ42/43, whereas control (SP stage 0) specimens did not.

Fig.16

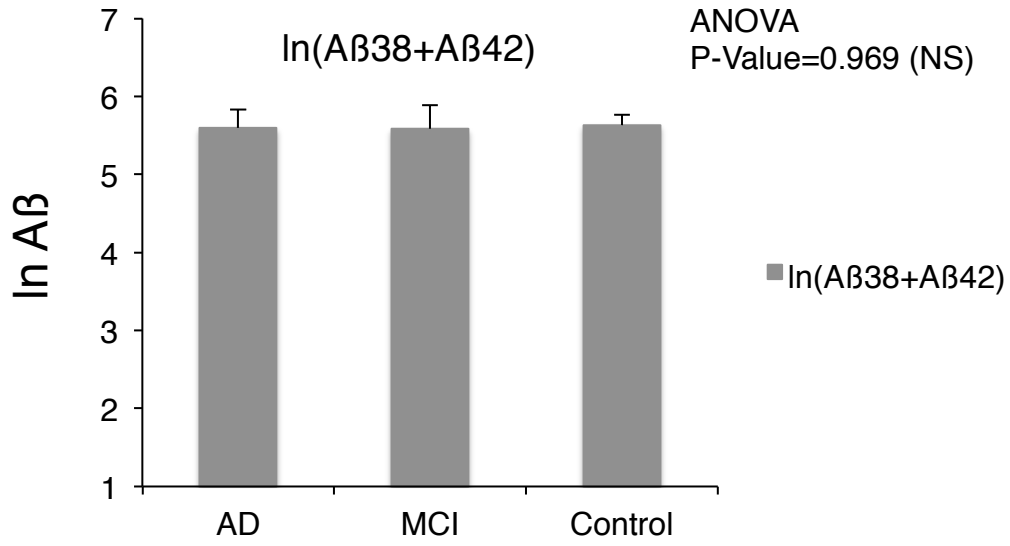

Figure 16. The raft-associated γ-secretase prepared from AD, MCI and control cortices was incubated with βCTF for 2h at 37˚C. Produced Aβs were quantified by Western blotting using specific antibodies. The amounts of ln(Aβ38+Aβ42) between controls, AD and MCI brains are not significantly different (ANOVA, *P*=0.969), ruling out selective inactivation of γ-secretase in MCI/AD.

Fig.17

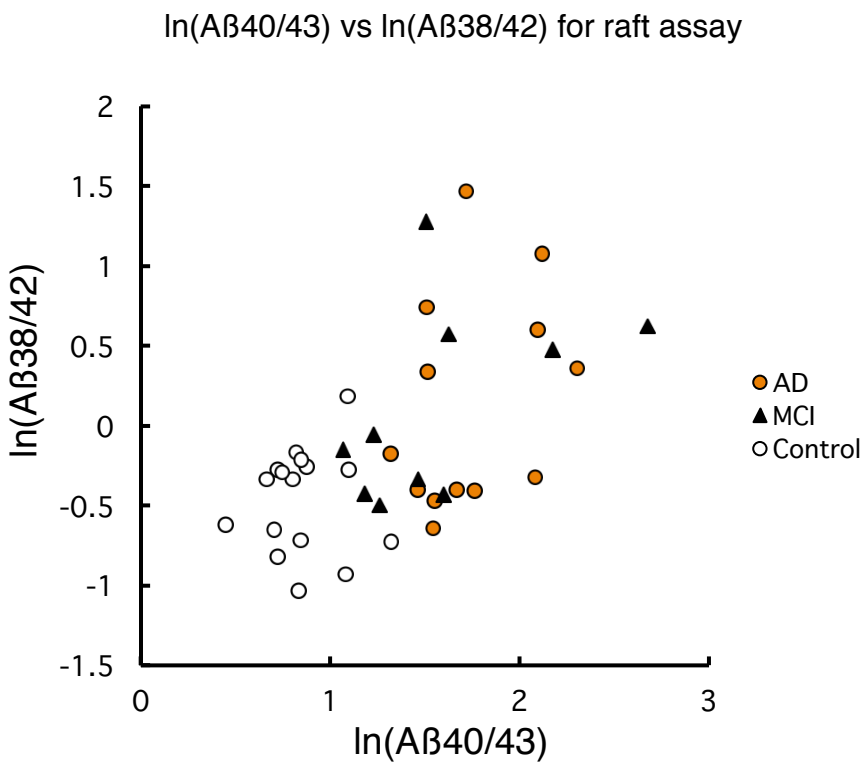

Figure 17. Ln(Aβ40/43) vs ln(Aβ38/42) plot based on direct quantification of raft-associated γ-secretase activity. The raft-associated γ-secretase prepared from control and MCI/AD brain specimens was incubated with βCTF for 2h at 37˚C (see materials and methods). Produced Aβs were quantified by Western blotting using specific antibodies. This plot distinguishes between control subjects and MCI/AD patients (Aβ40/43 for control vs MCI/AD, $P<0.001$; Aβ38/42 for control vs MCI/AD, $P=0.001$; Welch's t-test). MCI/AD plots [closed triangles (n=10) and orange circles (n=13), respectively] are as a whole a little distant from the origin, whereas control plots [open circles (n=16)] are close to the origin.

Table 1

Table 1. Apparent *K*m (*K*app) and *V*max for each Aβ species

			% of total Aβ	
	*K*m (*K*app, nM)	*V*max (AU)	0.5 μM C99-FLAG	2.5 μM C99-FLAG
Aβ40	407.91 ± 45.26	205.38 ± 32.41	44.80 ± 8.02	27.43 ± 6.62
Aβ42	608.85 ± 66.49	172.87 ± 86.41	23.20 ± 7.73	25.53 ± 6.84
Aβ43	724.82 ± 76.68	179.85 ± 32.85	19.69 ± 0.84	27.95 ± 2.61
Aβ45	788.22 ± 76.17	56.18 ± 8.89	5.73 ± 0.23	8.77± 1.10
Aβ48	753.99 ± 141.68	24.87 ± 2.75	2.59 ± 0.70	3.91 ± 0.54
Aβ49	933.17 ± 208.28	41.48 ± 12.49	3.98 ± 0.39	6.40 ± 1.22

Varying amounts of C99-FLAG were incubated in 0.25% CHAPSO lysate from microsomal fraction of CHO cells for three hours. Protein samples were subjected to western blotting using 82E1. Intensity of each Aβ species was plotted as % of intensity of 50 pg synthetic Aβ45 (see Fig. 3B). Percentages of total Aβ for each Aβ species were calculated as % of sum of Aβ species generated at 0.5 and 2.5 μM C99-FLAG. Data represent the mean ± SD (n = 3).

Table 2

Table 2. Effect of FAD mutations of APP on apparent *K*m (*K*app) and *V*max for Aβ and AICD

	Aβ		AICD	
	*K*m (*K*app; nM)	*V*max (pM/min)	*K*m (*K*app; nM)	*V*max (pM/min)
WT	507.93 ± 26.45	433.53 ± 51.94	468.72 ± 129.26	419.62 ± 19.39
V717F	682.80 ± 42.61	394.33 ± 41.43	598.63 ± 146.40	365.52 ± 23.36
T714I	352.43 ± 19.97	134.10 ± 24.83	294.33 ± 121.70	191.63 ± 66.57
I716F	937.20 ± 143.59	252.46 ± 29.71	903.93 ± 300.40	275.51 ± 98.79

Defined amounts of mtC99-FLAG substrate were incubated with 0.25% CHAPSO lysate from microsomal fraction of CHO cells for three hours. Protein samples were subjected to western blotting with synthetic Aβ and *E. coli*-expressed AICD (see text) being authentic standards. Aβ and AICD produced from wtC99-FLAG or mtC99-FLAG were visualized with 82E1 and UT-421, respectively, and their intensities were quantified (see Fig. 5A). Data represent the mean ± SD (n = 3).

Table 3

Table 3. Subject characteristics and CSF concentrations of Aβs

	Control	MCI	AD	ANOVA****p-value
Age (years)	74.9±7.5	72.5±6.6	72.3±8.2	
N (male/female)	21 (10/11)	19 (7/12)	24 (7/17)	
MMSE score	28.7±1.9	25.7±2.6*	19.6±3.3*	
ApoE ε4	3 (14.3%)	10 (52.6%)**	14 (58.6%)**	
Aβ38 (pM)	594.5±286.3	669.4±247.6	760.57±269.4	
Ln(Aβ38)	6.28 ±0.46	6.44 ±0.38	6.56 ±0.41	NS
Aβ40 (pM)	1607.9±712.9	1939.5±698.0	2292.6±799.6***	
Ln(Aβ40)	7.28 ±0.47	7.51 ±0.38	7.68 ±0.35	0.007
Aβ42 (pM)	133.1±53.4	83.2±49.4***	90.3±40.1***	
Ln(Aβ42)	4.80 ± 0.47	4.25 ± 0.60	4.40 ± 0.47	0.004
Aβ43 (pM)	11.8±5.7	6.8±5.6***	7.0±4.6***	
Ln(Aβ43)	2.32 ± 0.60	1.59 ± 0.86	1.76 ± 0.62	0.004

*P <0.01; Bonferroni's t-test for between control and MCI or AD (p=0.0012 for control vs MCI, p<0.001 for control vs AD, p<0.001 for MCI vs AD)
**2 MCI subjects were homozygous for ε4, while 4 AD subjects were homozygous for the allele.
***P <0.05; Dunnett's t-test after log-transformation for comparing between control and MCI or AD
****p-value of analysis of variance after log-transformation